



Norwegian University of
Science and Technology

Surface volume control through continuous surveillance of drilling data

Tone Carlsen

Petroleum Geoscience and Engineering

Submission date: June 2017

Supervisor: Pål Skalle, IGP

Norwegian University of Science and Technology
Department of Geoscience and Petroleum

Acknowledgement

Foremost, I would like to thank Professor Pål Skalle for his expertise, advices and support throughout this project. I would also like to thank the Department of Geoscience and Petroleum at NTNU for providing Real Time Drilling Data (RTDD) which I needed for developing and testing of my model, and, for providing expertise from several professors. Also, I give a big thanks to Anisa Noor Corina, Sigve Hovda and Isak Swahn for providing an interactive tool for viewing, reading and managing of the RTDD, and for them sharing their knowledge related to the data acquisition process.

In addition, I would like to thank Diskos, the Norwegian National Data Repository for Petroleum data, for providing additional RTDD to the local NTNU database, drilldb. A final thanks goes to another master student at NTNU, Clement Pierre Jean Donne, for good collaboration on the data cleaning process.

This master project has been very challenging and interesting, and it has been a great learning experience, where I have gained knowledge I will take with me in my future work.

Summary

When a new well is being drilled, volume control should be among the most important focus areas for the drilling crew. In every drilling operation, pressures exerted from the formations need to be controlled and overbalance in the well must be maintained. If any pressure barriers fail, for instance by insufficient drilling fluid density, an underbalanced situation arises, and formation fluids will slowly start moving into the well and “kicks” can occur. When kicks fail to be detected by the drill crew at surface, they may develop into a disaster, where both human lives and environment are put at risk.

Lost circulation is another consequence from not maintaining the correct pressures inside the well bore. If the hydrodynamic pressure downhole becomes larger than the formation breaking pressure, fractures are induced, and drilling fluid will start flowing into the fractures, reducing volume in the tanks, and, but seldom, reducing hydrostatic pressure in the well. In a worst-case scenario, this could develop into a kick situation as well.

The first part of this master thesis considers theory related to volume control, with main focus on lost circulation and kicks, and under which circumstances they may occur. In addition, previous research relevant to loss- and influx detection by monitoring RTDD parameters on the rig, is presented. The earlier volume control problems are detected, the lower the kick volume becomes, and the more time the rig crew gets to handle the kick in an appropriate and safe way.

The main part of this thesis is related to a mathematical model that intends to describe how the active tank volume is affected by typical drilling operations on a rig. This model takes in RTDD from a well (hereby named well 1A) on the Statfjord field, and compares the observed active mud tank levels on the rig to its theoretical modelled values. By doing so, it can detect when the observed mud level is deviating from the theoretical, and thus detect possible volume control related incidents. The final well report from well 1A was used for supporting the results of the model.

When tested on a drilled interval in well 1A on the 8th of February 2006, the model managed to detect loss of mud into the formation. The losses were confirmed from the final well report in only one of the two cases. In other words, the model detected unreported losses.

For further work, several modules of the model should be updated and more parameters included. Also, it should be tested on more wells -preferably wells with kick incidents- to better check model performance abilities. A final improvement would be to make the model more user-friendly and automatic, for instance by implementing it in MATLAB.

Sammendrag

Under boring av en petroleumsbrønn er det alltid viktig å ha stort fokus på volumkontroll. I enhver boreoperasjon må man hele tiden ha kontroll på trykkene nede i brønnen, og at disse alltid er i overbalanse mot formasjonen. Dersom noen av barrierene svikter, for eksempel ved for lav tyngde på boreslammet, kan formasjonsvæske begynne å strømme inn i brønnen og «brønnsparke» kan oppstå. Dersom disse «brønnsparke» ikke registreres av boremannskapet på riggen, er sjansen for en katastrofe stor, der både menneskeliv og miljø blir satt i fare.

Tap av sirkulasjon er en annen konsekvens av å ikke balansere trykkene i brønnen riktig. Dersom det hydrodynamiske trykket nede i brønnen blir større enn fraktureringstrykket, kan formasjonen begynne å slå sprekker, og borevæske vil begynne å strømme inn i disse. Dersom ikke dette tapet stoppes, kan store mengder borevæske forsvinne inn i formasjonen, og redusere hydrostatisk trykk i brønnen deretter. I verste fall kan dette også føre til en «brønnsparke»-situasjon.

Første del av denne masteroppgaven tar for seg tidligere forskning relatert til volumkontroll, og hvordan RTDD (sanntids boredata) kan brukes til å detektere uønskede volumendringer i slamtankene på boreriggen. I tillegg presenteres teori relatert til volumkontroll, der hovedfokuset ligger på tapt sirkulasjon samt «brønnsparke», og hvordan disse oppstår.

Hoveddelen av denne oppgaven omhandler en matematisk modell som forsøker å beskrive hvordan nivået i de aktive slamtankene påvirkes av typiske boreoperasjoner som gjennomføres på en rigg. Modellen tar inn RTDD fra en tidligere boret brønn på Statfjordfeltet (heretter kalt brønn 1A), og sammenligner observerte slamtanknivåer på riggen med teoretisk beregnede verdier. På denne måten kan modellen detektere når observert slamnivå avviker fra det som teoretisk kunne forventes, og advare om mulige problemer relatert til volumkontroll. Endelig brønnsrapport fra den aktuelle brønnen ble brukt til å underbygge modellens resultater.

Da modellen ble testet over et boreintervall i brønn 1A den 8. februar 2006, greide den å detektere tap av boreslam til formasjonen. Tapet ble bekreftet gjennom den endelige brønnsrapporten. I tillegg greide modellen å detektere urapporterte tap.

Videre arbeid med modellen er hovedsakelig relatert til å oppgradere den til å kunne ta inn flere parametere, som vil gjøre den mer nøyaktig. I tillegg burde den testes på flere brønner -aller helst brønner med problemer relatert til volumkontroll- slik at ytelsen kan sjekkes bedre. En siste forbedring vil være å gjøre den mer brukervennlig og automatisk, ved å implementere den i for eksempel MATLAB.

Table of contents

Acknowledgement.....	iii
Summary	v
Sammendrag	vii
1. Introduction.....	1
2. Previous work on volume control and RTDD	3
3. Kicks - increased tank volume	7
3.1 Causes.....	8
3.2 Detection	11
3.3 Prevention	14
4. Losses.....	17
4.1 Causes and detection	18
4.2 Prevention and diagnosis	21
5. Model of mud pit volume.....	25
5.1 Basic concept behind model	25
5.2 Parameters	29
5.2.1 V_{pit}	29
5.2.2 V_{in} and V_{out}	31
5.2.3 $V_{cuttings + film}$	33
5.2.4 Determining filling and emptying volume each time the pump is turned off/on (V_{pump}).....	44
5.2.5 $V_{adjustments}$	50
6. Cases for testing model.....	53
6.1 Existing database.....	53
6.2 Diskos.....	55

6.3 Cleaning of data and categorization	56
6.4 Selection of RTDD-files	59
7. Model evaluation	61
8. Self-assessment	67
8.1 Model performance	67
8.2 Data quality and uncertainty.....	69
8.3 Future work → Improvements of thesis work on basis of self-assessment.....	70
9. Conclusion	71
10. Nomenclature.....	73
11. Abbreviations	75
12. References.....	77
13. Figures	79
14. Tables.....	83
Appendix A: U-tube effect.....	85
Appendix B: Log viewer template	86
Appendix C: Capacities of drill pipes	88
Appendix D: Casing sizes	89

1. Introduction

Technological developments over the last decades have made it possible to collect and store huge amounts of well data gathered during drilling operations. The well data is valuable for the industry for several reasons, as they can:

- Provide an improved understanding of the drilled geology
- Increase drilling performance
- Provide general experience transfer
- Contribute to less non-productive time (NPT) and with that; lower drilling costs.

In this master thesis, real-time drilling data (RTDD) will be used for analytical purposes related to volumetric unstable wells. Two of the most time-consuming failures include influxes and losses, and they will be the main focus area. The goal is to discover patterns on how such failures occur and are handled, and to use this information on preventing similar, future incidents.

From well data it is possible to observe which failures occurred most frequently, and why they occurred. This can be used for predicting, detecting and avoiding failures and non-productive time (NPT) in future operations. My approach will therefore be to first learn more about the selected failure cases; kicks and lost circulation. Since well data is necessary for investigation purposes, an introductory task will be to search for, gather and store real-time drilling data (RTDD) from the Norwegian Petroleum Directorate's (NPD) database, Diskos. In order for the RTDD to be applicable with NTNU's local database, Drilldb\$, the data have to be cleaned and prepared before they are downloaded. The final step will then be to evaluate the data; first at a high level where they will be categorized and characterized, then the failure cases related to influx and losses will be found and presented. They will then be analysed to evaluate what caused them, and a model will be made that tries to detect such failures through RTDD and the active mud tank. Lastly, the model will be tested on real wells from the drilldb-database.

2. Previous work on volume control and RTDD

Several studies have been done on using RTDD for continuous downhole monitoring while drilling. The benefits are many; drilling problems can be reduced and better decisions can be made while drilling, as the driller is continuously updated on the state of the well. The basic concept behind most of the studies, is a model that takes in real-time data, and creates an ideal operating envelope for the drilling team to follow. If some of the parameters start to deviate from the proposed model, the drilling team will be notified immediately and the correct actions can be taken.

One of these studies was performed by the International Research Institute of Stavanger (IRIS), which developed a model driven by RTDD from the rig. The calculations in the model are solved and calibrated real-time, and based on the actions of the driller. It considers parameters from both downhole and surface sensors, and calculates an expected range of values for these (see Figure 2.1). Some of the parameters include hydraulic pressures, torque, hook load, mud pit levels, cuttings location and standpipe pressures. By doing so, the drillers are provided with guidelines on checking the data quality, and they can detect symptoms of poor hole conditions that could cause drilling problems at a later stage (Chmela et al.).



Figure 2.1: The principle behind IRIS' model, which compares real-time sensor data with calculated model data (Chmela et al.).

The sensor outputs are calculated every second; as soon as the RTDD is detected on the rig. This applies for all drilling activities, like tripping, drilling and circulating. It is therefore possible to do continuous comparison of the measured values from the sensors, and the expected values from the model. Because of this, any deviations or problems can be detected at the earliest, possible time, and failures like lost circulation and kicks can be avoided.

The software developed from this model, has already been tested on 15 wells in five different fields located in the North Sea. Every major event was warned to the drilling crew; situations that occurred instantly (like having the drillstring stuck into a cuttings bed while pulling out) were warned about 30 minutes before the failure, incidents with medium detection-time were warned typically 6 hours before they were to occur, and downhole changing conditions that develop slowly, were detected up to one day in advance.

Behind the software is a computer system that systematically analyses RTDD to monitor the downhole conditions. It is based on five principles:

1. Continuously evaluates the conditions of the well by running real-time physical models of the drilling process.
2. Detects all current well conditions that can be used for calibration of the physical models.
3. Performs a continuous global calibration of the different physical models, in order to match the recorded relevant well conditions.
4. Detects if the current well conditions are deviating from what is considered normal.
5. Warns key personnel if drilling conditions are getting poorer, or will cause limitations to the drillability of the well.

Several drilling parameters are monitored, including the active volume tank, and symptoms behind lost circulation and kicks can be detected. By comparing the return flow rate and injection flow rate, a decrease of pit volume can be noticed, and lost circulation warned. Contrarywise, influx into the well can be detected by evaluating the total fluid volume in the system and gains in the active pit volume. However, other pit volume variations also need to

be considered, like fluid flowback/inflow from/to the pumps (see Figure 2.2) and loss of mud with cuttings in the shale shaker.

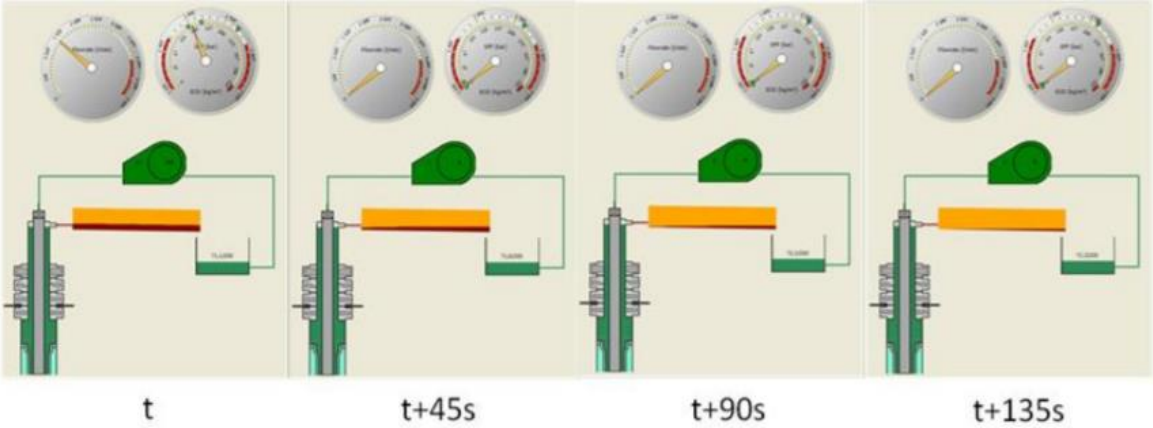


Figure 2.2: It can take several minutes from the pumps are shut down until all of the fluid stored in the surface lines flows back to the active tank, which causes an apparent gain (Cayeux et al., 2012).

By taking all of the mentioned variables into account, the software managed to detect the beginning of a kick situation in one of the test wells. During a connection (while drilling), the system detected an abnormal increase in the active mud pit (see Figure 2.3), six minutes after the pumps were stopped (two minutes after the pit level should have stabilized). The drilling crew could therefore initiate necessary measures at an early stage, which prevented a possible kick incident (Cayeux et al., 2012).

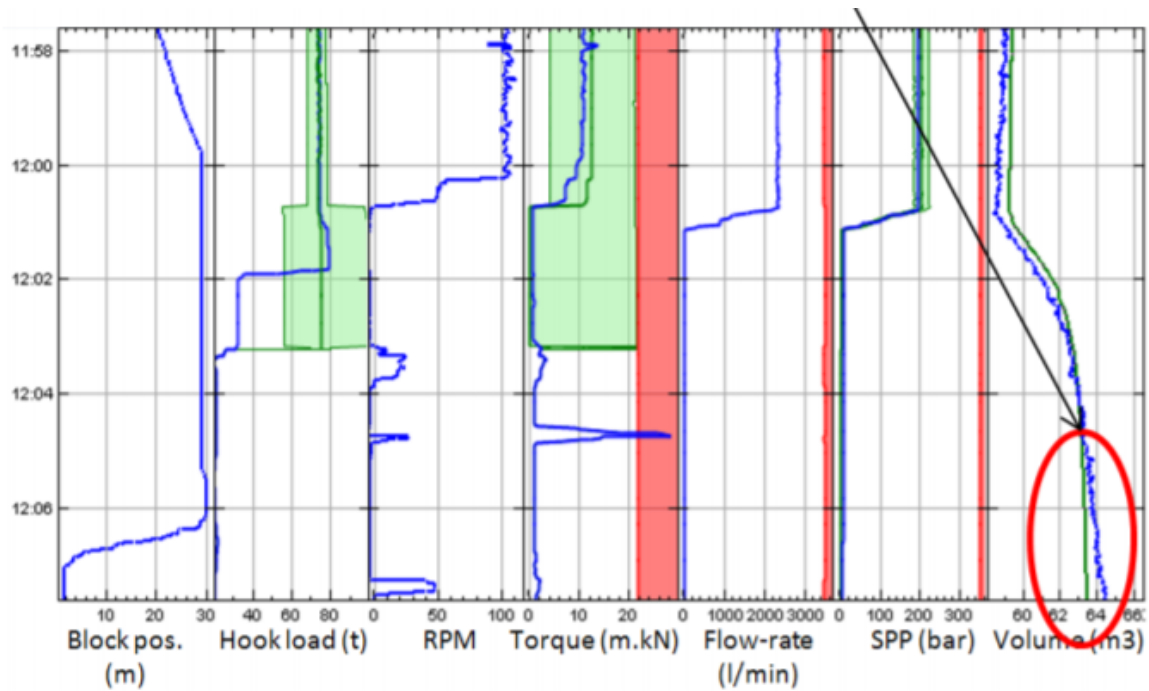


Figure 2.3: The red circle indicates where the models (green graph) discover an abnormal mud level increase when compared to the measured tank volume (blue graph) (Cayeux et al., 2012).

It is evident that the topic of this master thesis is highly relevant for the drilling industry, and that much time and effort is put into research of ways to take more advantage of RTDD in volume control. However, as models have limitations on their accuracy and reliability (at least for now), it is important to be aware of the fact that models can only give symptoms, not a diagnosis. The drilling team still needs to interpret parameters and indications from the well and not rely fully on model calculations.

3. Kicks - increased tank volume

An important aspect of volume control is to ensure that the well is taking the correct amount of drilling fluid at all times. As soon as the well is taking either too much, or too little fluid than is injected, it is a strong indicator of volume control problems. If the failure is related to influx of formation fluid, the change in volume level is small at an early stage.

Influx occurs when the wellbore pressure becomes lower than the formation pressure, and the formation is permeable. “Kick” is another name commonly used by the industry. In this chapter, different indicators of kicks will be presented and theory related to volume and pressure control. The chapter is divided into:

- Causes
- Detection
- Prevention

All three aspects are relevant when analysing kick incidents from RTDD. By knowing what causes kicks and from which parameters they can be detected, it can be seen how RTDD are important for kick handling. Kicks can also be prevented from the same method; when analysing RTDD during a drilling operation, several parameters can give indications about an imminent kick situation. The most important RTDD-parameter for kick detection is the active tank volume (TVA) when combined with theory from volume control, steel displacement volumes and hole information. High-pressure zones are typical areas where kicks are likely to occur, and can also be detected from RTDD-parameters. By monitoring the drilling rate (Rate of Penetration, ROP), it can be possible to detect such transition zones, as gradual increases in ROP can be an indication of a high-pressure zone. Other RTDD-parameters relevant for kick detection are mud-out flowrate, pump pressure, pump strokes per minute (SPM) and gas content in mud.

3.1 Causes

There are several warning signs and kick indicators that can be observed and interpreted before a kick escalates in size. These are known as leading indicators of kick, and are early signs that a kick is potentially occurring. Such early warnings can help prevent an influx, as long as they are noticed. However, all the parameters need to be monitored collectively, as one indicator alone is too vague for making an interpretation. Some of these leading indicators include improper fluid density (Nayeem et al., 2016):

- Too low drilling fluid density
- Insufficient drilling fluid level in the well
- Swab and surge
- Unexpected abnormal high pressure zone
- Lost circulation

Formation fluid downhole is kept in place as long as the hydrostatic pressure (eqn. 3.1) in the well is larger or equal to the formation pore pressure, seen in eqn. 3.2:

$$P_{hydrostatic} = \rho_{mud} * g * h \quad (3.1)$$

$$P_{hydrostatic} \geq P_{formation} \quad (3.2)$$

This can be maintained by securing correct drilling fluid density. As soon as the hydrostatic pressure becomes less than the formation pore pressure (eqn. 3.3), formation fluids will start entering the well, and a kick situation arises.

$$P_{hydrostatic} \leq P_{formation} \quad (3.3)$$

However, if the density of the drilling fluid becomes too high, pressure exerted from the hydrostatic column could induce fractures in the formation. This will cause leakages of drilling fluid into the formation and lost circulation would occur. As a result, the fluid level in the well will fall, and hydrostatic pressure is reduced according to equation 3.1 (also see Figure 3.1). The drilling fluid level inside the well is also dependent on the amount of steel

(drill pipe, BHA, etc.) present in the hole. When performing tripping operations, where steel is either removed or added into the well, it is important to add/remove the equivalent volume of drilling fluid in the well to maintain proper hydrostatic pressure.

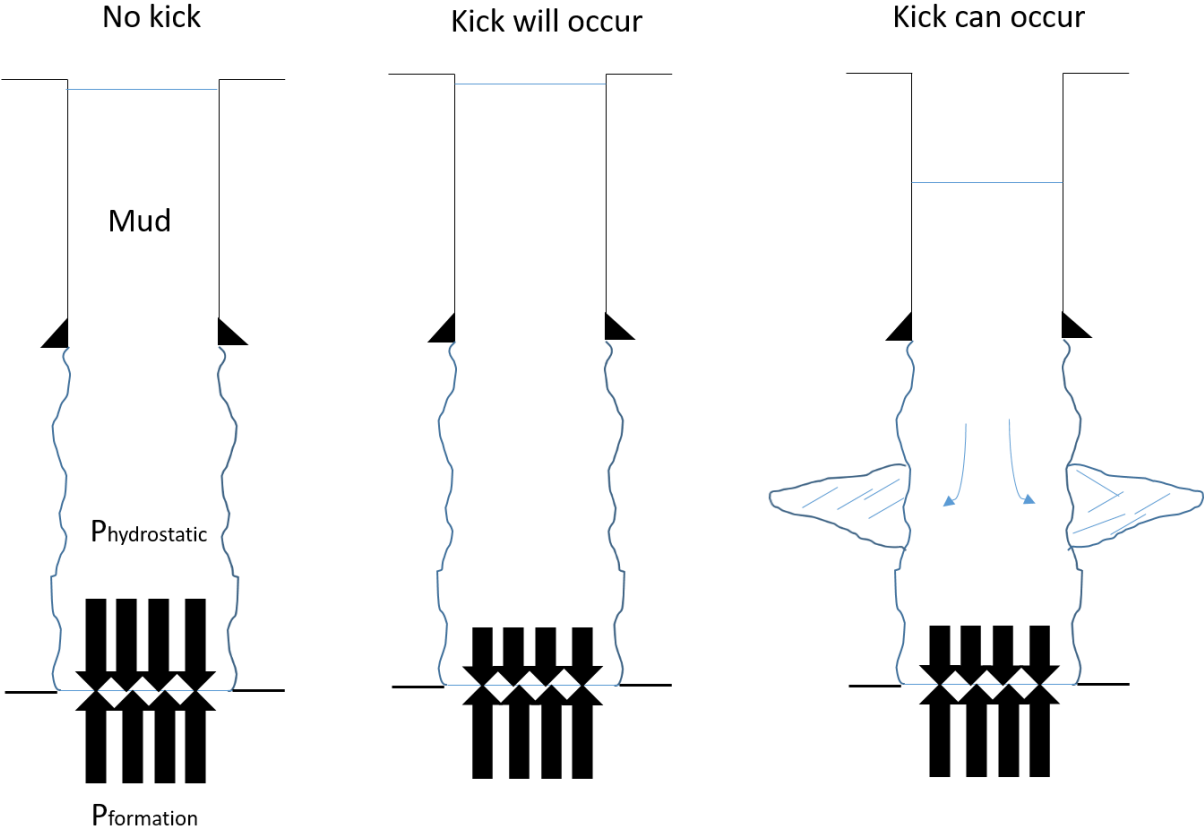


Figure 3.1: Kicking well: Left: a balanced situation where the hydrostatic pressure is higher or equal to the formation pressure; no influx. Middle: kick situation, where the hydrostatic pressure is too low to withstand the formation pressure. Right: lost circulation.

When performing tripping operations, one also needs to be aware of surge and swab pressures. Surge happens if the drill string is run too fast inside the hole, so that the pressure below the bit increases as a result of the movement. This can make the bottom hole pressure too large and cause lost circulation. Swab, on the other hand, happens when the drill string is pulled out of the hole too fast. Friction along the wall and pipe movement cause a pressure reduction below the bit, which lowers the hydrostatic pressure. It is therefore important to perform tripping operations with controlled velocities, and be aware of surge/swab margins.

Abnormal high pressure zones are often associated with kicks, as these are formations with higher pressures than expected at a certain depth. The definition of such zones is pressures that have an equivalent mud weight greater than normal conditions, where normal conditions are considered hydrostatic pressure of brine (Mitchell and Miska, 2010). Therefore, if abnormal high pressure zones are hit during drilling with insufficient mud weight, influx could enter the well. This is, however, dependent on the porosity and permeability of the rock.

Another leading kick indicator, not related to fluid density, is a drilling break. This is characterized by an abrupt increase in bit penetration rate (see Figure 3.2) which can indicate that the rock type has changed (not to be confused with a gradual increase, which is the case for abnormal pressure zones). It can also indicate that this new rock type has the potential to kick compared to the previously drilled rock section (sandstone formations are more likely to kick than shales because of different permeability and porosity properties). However, even if a drilling break is encountered, it is not certain that a kick will occur. The only information one can interpret from it is that a formation with kick potential is being drilled. It is therefore recommended practice to drill 1 - 1,5 meters into the new formation before performing a flow check.

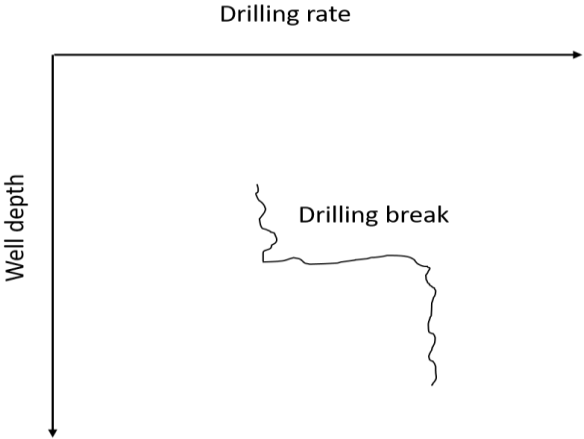


Figure 3.2: Example showing how a drill break looks on the Drilling rate vs. well depth plot.

3.2 Detection

Lagging indicators are another type of kick indicators which include chemical and physical changes that occur in the wellbore after an influx has entered the well. In other words, they can be used for detection and give information about the influx as well as the severity of it. This type of information cannot help preventing an ongoing kick, but could be used in order to avoid it becoming a blowout. These lagging indicators are divided into two groups, primary and secondary lagging indicators, based on their importance in kick detection (Nayeem et al., 2016) & (Lake and Mitchell, 2006):

Primary lagging indicators of kick:

- Increase in mud pit volume
- Increase in flow-rate
- A well that flows after pumps are shut down

Secondary lagging indicators of kick:

- Changes in drill string weight
- Changes in pump pressure (decrease when pump stroke increase)
- Changes in return mud properties/gas cut

The three warning signs of primary importance to kick detection are vital to notice, and take seriously if they were to occur. When the mud pit volume increases on the rig without any controlled actions being performed by the drill crew, it could be a strong indication that formation fluid has entered the well. This influx volume displaces mud that is already in the wellbore, and forces it out of the well, which results in the pit gain (see Figure 3.3 for visualization).

An increase in flow-rate at surface is a key indicator that a kick is moving up the wellbore if the pumps simultaneously pump at a constant rate. This because an increased flow-rate could mean that the formation is helping the rig pumps move drilling fluids up through the annulus.

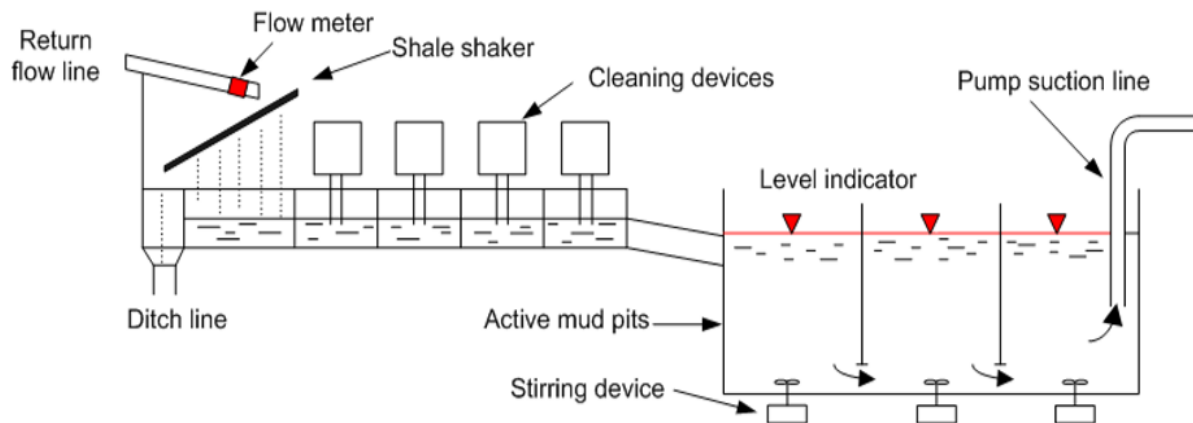


Figure 3.3: An overview of the circulation system showing how the mud pits are connected to the well. The fluid level in the mud pits is monitored to check for volume increases by the level indicators (Brechan, 2015).

The last primary lagging indicator of a kick is if the well flows with mud pumps shut down. Since the mud pumps are off, flow in the wellbore is driven by formation fluids moving up through the annulus. However, there is one exception that could cause flow with pumps off; when the mud inside the drill string is considerably heavier than the one in the annulus, for instance by use of a slug pill. One therefore needs to be aware of the symptoms when using a slug pill.

Indications of a changing drill string weight is a secondary lagging indication of kick. Since the drilling fluid inside the well provides a buoyant effect on the drill string, it helps reduce the string weight held by the derrick at surface. Heavier drilling fluids provide more buoyancy forces than less dense drilling fluids. Because of this, a kick with low density would cause a lighter mud, and hook load at surface would become bigger as the buoyancy force reduces. However, this effect is not always large enough to be observed at the surface (see hook load plot in Figure 3.4).

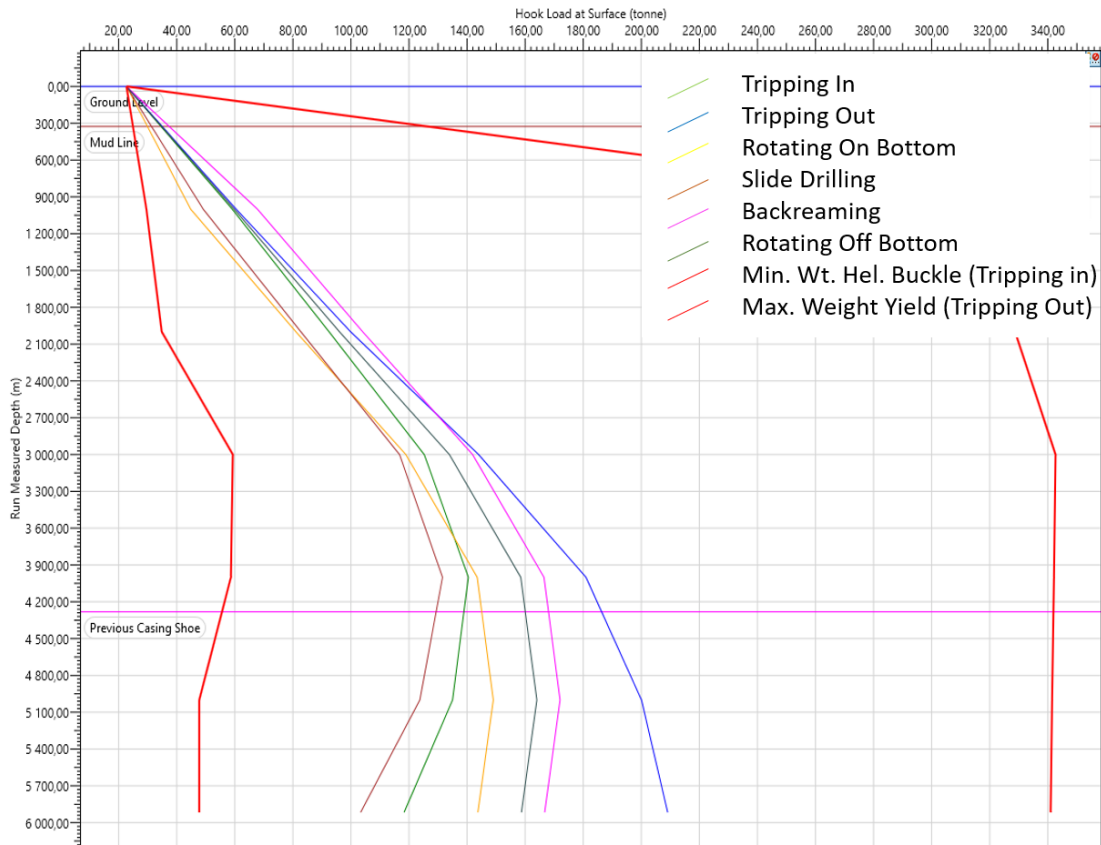


Figure 3.4: An example of a hook load plot. In the event of an influx, the hook load will increase as a reaction to smaller buoyancy force provided by the lighter mud in the wellbore. (WellPlan™ software).

Another secondary lagging indication of kick is when pump pressure decreases while number of strokes increases. When an influx enters the well it can cause the mud to flocculate, which will increase the pump pressure. As more low-density influx flows in, it displaces the heavier mud already in the wellbore. This causes the pump pressure to start decreasing. The annular fluid will after some time become less dense, and the mud inside the drill string tends to fall down, which causes the pump speed to increase. However, this symptom can be initiated by other sources as well, and it is important to exclude that the reason is a kick.

The last secondary lagging indication of a kick is when there are changes in the properties of the return mud (density of mud is reduced). This can be caused by either core volume cutting, aerated mud circulated from the mud pit and down the drill string or connection air. Reduced mud weight often occurs when drilling through formations which contain gas. However, the density reduction is seldom big enough to affect the bottom hole pressure significantly (Mitchell and Miska, 2010).

3.3 Prevention

Improperly filling of the well during tripping operations is one of the predominant causes of kicks. Tripping is a term used to describe the operations where drill pipe is either pulled out of the hole (POOH) or run inside the hole (RIH). These trips are made while the circulation system is shut off. Therefore, removal or addition of steel pipe out of/into the well will affect the drilling fluid level. For instance, if one stand of drill pipe (see Figure 3.5) is pulled out of the hole, the fluid level in the well will fall according to the volume of steel removed. In the same way, when running a stand of drill pipe, an equivalent drilling fluid amount will have to be removed from the well. However, if the theoretical steel displacement volume does not match the actual volume needed to fill (or take out) the hole, there is a large possibility of a well control problem. One reason for the well not taking the right amount after pulling the drill pipe out, could be an influx, which increases the fluid volume in the well so that less mud is needed to refill. On the other hand, if drill pipe is run in the well and the return fluid is less than the steel volume lowered, there are reasons to believe that lost circulation is the reason.

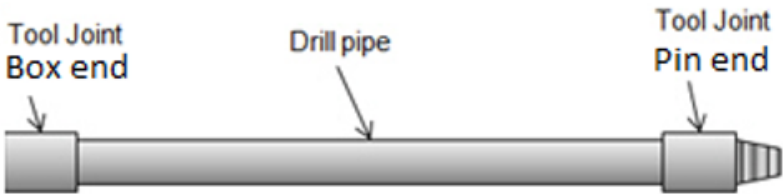


Figure 3.5: A single drill pipe. Each end consists of a tool joint; one pin end and one box end, which will affect the volume displacement in mud (Brechan, 2015).

The most common tool used for such volume control at surface today, is a trip tank. Trip tanks are small and usually designed to hold only 1.6 to 2.4 m³ of drilling fluid (see Figure 3.6). Gauge markers are set at every 0.16 m³ so that it is easy to continuously monitor volume changes that occur while tripping in and out of the well (Mitchell and Miska, 2010). In this way, the theoretical displacement volumes can be compared to the true ones from the trip tank.

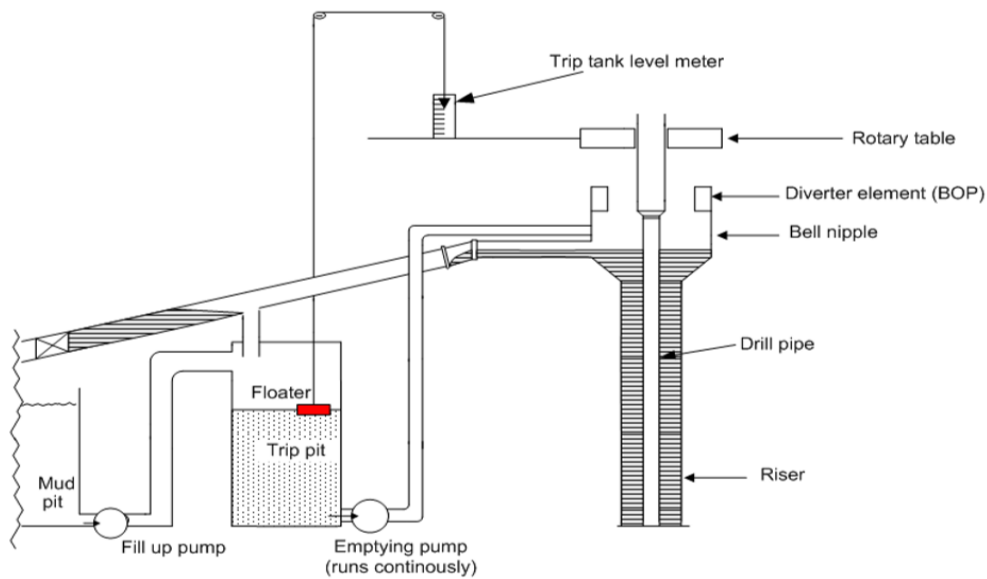


Figure 3.6: Trip tank arrangement on a drilling rig (Brechan, 2015).

In any event where those two volumes are not equal, or within a pre-determined safety limit, a visual flow check should be performed to check for influx. If the well flows, shut-in procedures need to be initiated and appropriate well control methods applied. If the well does not flow, this indicates that there is still overbalance between the formation pressure and wellbore pressure. However, there are still chances that a kick is travelling up the wellbore. The risk is especially large if the influx consists of gas, which expands on its way up. It is therefore important to lower the bit to bottom and circulate bottoms-up to check for gas (School of Petroleum Engineering, 2014).

The trip tank system can be arranged in three different ways; a passive type, semi-passive type or an active type (see Figure 3.7). The passive arrangement is based on the u-tube principle (see Appendix A), and no valves or pumps are needed. In the semi-passive arrangement, mud is fed to the well by gravity forces. Here, the trip tank is placed above the preventer, which allows mud to flow controlled into the annulus by use of valves. The last trip tank arrangement is an active type, which uses a centrifugal pump to transport mud from the tank and into the well. This type of arrangement is widely used in the Norwegian petroleum industry today.

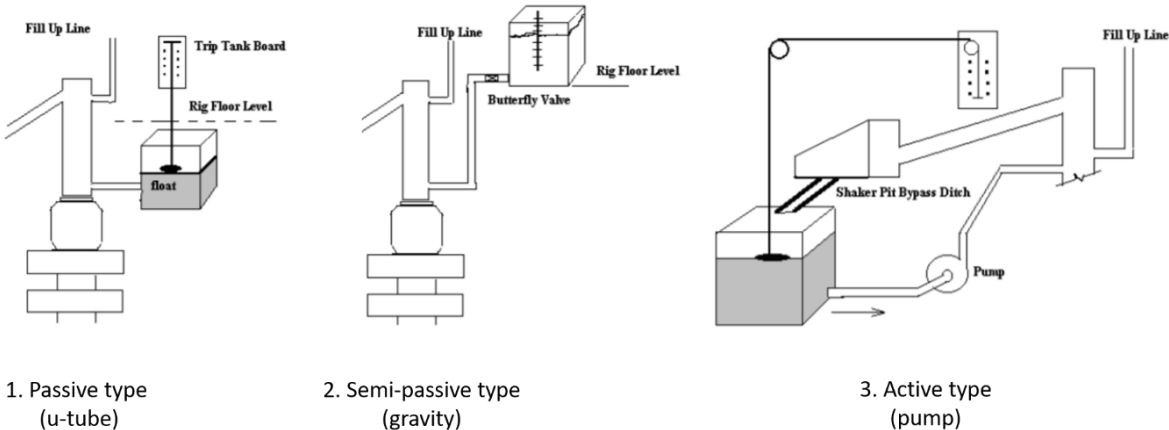


Figure 3.7: Overview of the three trip tank arrangements; 1. Passive type (based on the u-tube principle), 2. Semi-passive type (based on gravity forces) and 3. Active type (based on a centrifugal pump (School of Petroleum Engineering, 2014).

However, kicks can occur during other operations than tripping in and out. In such cases, the trip tank is disconnected, and the active mud pits are connected. Possible volume gains are now detected from these instead (see Figure 3.3). Operations that use the active mud pits for volume control includes drilling and backreaming.

4. Losses

Lost circulation occurs when less fluid is returned from the wellbore than what is being pumped into it. In other words, drilling fluid (usually mud or cement slurry) is lost to the formation through fractures (see Figure 4.1), which makes it one of the most troublesome and costliest downhole problems. It is estimated that hundreds of millions of US dollars are spent annually worldwide on direct or indirect lost-circulation problems (including materials, services and down-time). In worst case scenarios, the fluid level in the well can drop rapidly by hundreds of feet, which can result in loss of hydrostatic pressure and cause kicks. Losses and kicks are therefore related. These situations are challenging to handle, as well control methods that require circulation of kill mud are not very efficient. Another consequence can be reduced well productivity because of formation damage (Mitchell and Miska, 2010).

This chapter considers the causes of lost circulation, typical loss zones and remedial actions. The chapter is divided into:

- Causes and detection
- Prevention and diagnosis

The causes behind lost circulation are presented to increase the understanding on how pressures exerted to the formation can cause big downhole problems and how it relates to the surface mud tank level. Detection and prevention are also relevant aspects of lost circulation when considering the importance of RTDD. Parameters that can warn about possible lost circulation situations includes ECD, mud pit level (TVA) and ROP together with theory related to volume control.

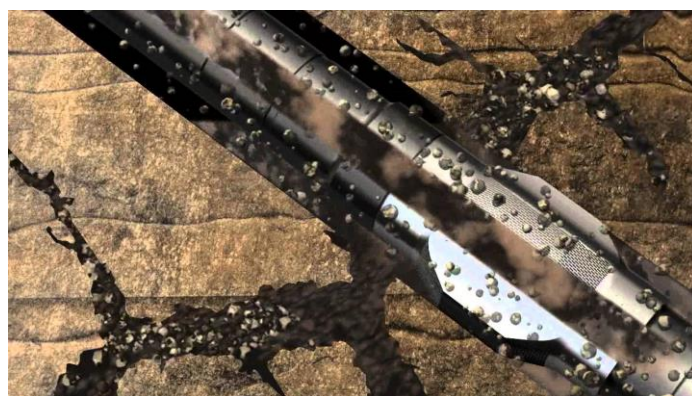


Figure 4.1: Lost circulation zone being drilled (Halliburton, 2013).

4.1 Causes and detection

Two conditions need to be present in order for lost circulation to occur:

1. A formation containing channels allowing passage of fluids from the wellbore
2. Positive pressure differential between the formation and the wellbore (the fracture pressure of the formation is smaller than the wellbore pressure (ECD))

Both of them must be present at the same time, although one of the two can dominate. For instance, if the formation is highly porous and permeable, a small overbalance will be enough to cause lost circulation. There exist four different zones/formations with specific characteristics that have higher potential of lost circulation (Mitchell and Miska, 2010).

These include:

- Permeable and porous zones
- Natural fractures
- Induced fractures
- Cavernous and vugular formations

Permeable and porous zones consist of rocks with high primary porosity and permeability. Formations with these characteristics are particularly at risk, because of the optimum flow conditions. Gravel beds, loose conglomerates, unconsolidated formations and highly depleted or shallow sandstones are typical structures of these zones (see illustration up in the left corner on Figure 4.2). When mud is leaking into the formations, a gradual drop in mud pit level is observed. If the leakage is not encountered, and drilling continues, partial or complete loss of returns is a possible consequence.

Natural fractures in sandstones, carbonates and shales can be related to lost circulation problems (see illustration down in the right corner on Figure 4.2). Secondary porosity and permeability cause good flow conditions from the well into the formations. The fractures can be both vertical and horizontal, based on the mechanical characteristics of the rock, burial depth and stress environment. A vertical fractured system will take increasing amounts of mud based on the drilling progress, and how many fractures are exposed. A horizontal system, however, will take gradually more mud as additional fractures are encountered and could result in a complete loss of returns.

Induced fractures are a result of human impact (see illustration up in the right corner on Figure 4.2). They occur as soon as the wellbore pressure exceeds the fracture gradient of the formation. Typical operations that cause such high pressures include too high pump rates/velocities, lowering pipe too fast (surge), breaking circulation or raising mud weights too high. Hydraulic fracturing also initiates fractures, however, this kind of operation is usually performed under controlled circumstances only. Once a fracture has been induced, fluid can flow freely from the wellbore into the formation if the pressure is high enough, and cause lost circulation. Induced fractures cannot be repaired, and lost circulation can also occur at a later stage, even after pressures are reduced.

The most severe lost-circulation problems occur when drilling through cavernous or vugular formations. These formations typically consist of limestones that have interacted with water, or other formations with secondary porosity. They are characterized by vugs and void spaces filled with oil or brine (see illustration down in the left corner on Figure 4.2). When encountering such formations while drilling, the drillstring can potentially fall freely through the open space and a sudden decrease in mud level is experienced. Depending on the size of the void spaces, everything from small losses to complete loss of returns are possible outcomes (Mitchell and Miska, 2010) (Gaurina-Medjimurec and Pasic, 2014).

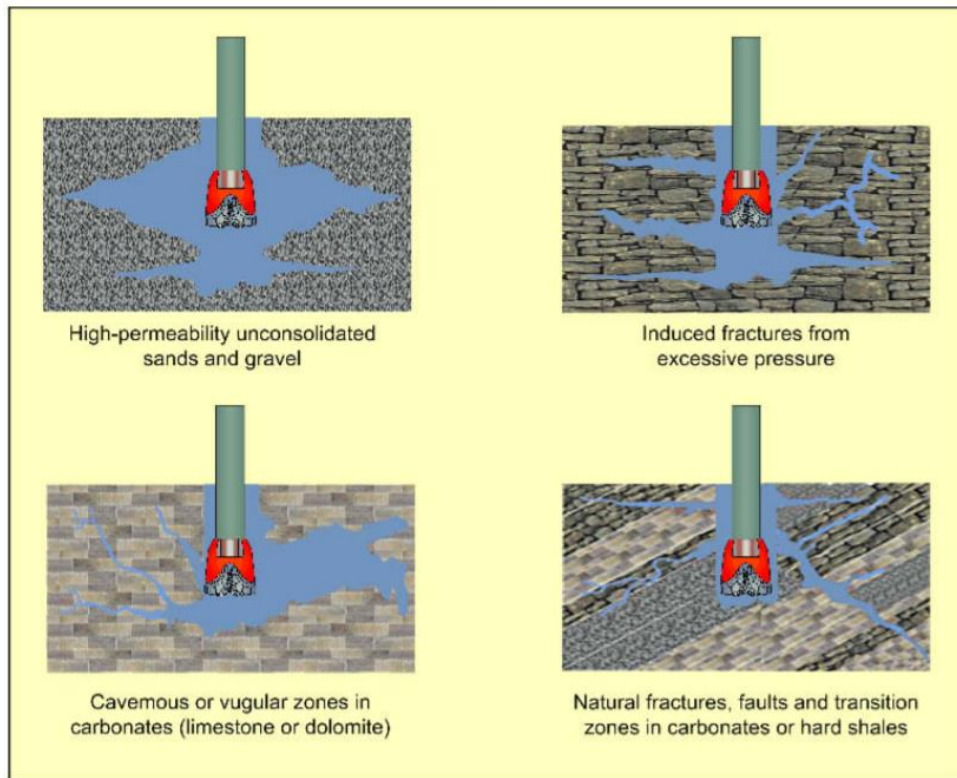


Figure 4.2: Overview of lost circulation zones (Gaurina-Medjimurec and Pasic, 2014).

Such zones can be revealed by monitoring RTDD. Rate of Penetration (ROP) can for instance give indications of transition zones between two formations with different properties (like hardness, porosity etc.) (more information can be found in chapter 3).

Furthermore, ECD can be used as an indication of drilling-induced fractures. When mud pumps are turned on, the ECD parameter will increase rapidly if the formation is fully intact. However, if fractures have been induced, the increase in ECD will be more gradual. This is explained by fluid flowing back into the well from the fractures, that will cause a more gradual increase in ECD (Lavrov, 2016a).

4.2 Prevention and diagnosis

Since lost circulation problems are expensive and time consuming, the most optimal solution would be to avoid them. There are several measures that can either minimize, or even prevent, lost-circulation problems. Most of them relates to controlling positive overbalance between the formation and the wellbore (fracture pressure – ECD). Choosing the right mud system is therefore of great importance. Mud density, viscosity, yield point and gel strengths all need to be kept low enough to prevent lost circulation, but high enough to ensure effective drilling and good hole cleaning. Especially, the viscosity needs to be maintained at a moderate level, as too high viscosities have a tendency to increase the ECD. High ECD can cause formation breakage, and lost circulation, even though mud weight is kept low.

Another important aspect of preventing lost circulation problems, is to maintain a continuous circulation; stopping and re-starting of the circulation system should be avoided and a steady pressure should be maintained downhole. This will minimize erosion of the exposed formation and hinder further instabilities.

Lastly, using available information about locations and potential loss zones can be valuable when planning the well trajectory, in order to avoid lost circulation zones (Gaurina-Medjimurec and Pasic, 2014) (Lavrov, 2016b).

Several methods can be used to diagnose lost circulation. When deciding which method should be used for a specific situation, three diagnostic steps are used:

- Determine at what depth the loss is occurring
- Describe what type of loss zone is present
- Evaluate severity of loss

Typically, loss zones are located near the casing shoe, not at the bottom, as one could expect. This is explained by the fracture gradient, which is often at its lowest in this area. When trying to locate a lost-circulation zone, different logging devices are used like temperature logs, radioactive-tracer tools and spinners. Temperature logs can detect loss zones based on temperature differences, when colder mud is being pumped (see Figure 4.3). Radioactivity can be used for tracing purposes. Two gamma ray logs can be run for comparison, where radioactive material is added before the second run. If losses have occurred, it is possible to observe a steep change of radioactivity at the loss zone. Lastly, a spinner survey can be run. A spinner is attached to the end of a cable, and run down to the suspected loss area. If the spinner spins/accelerates during mud movement, it indicates mud flow into the formation.

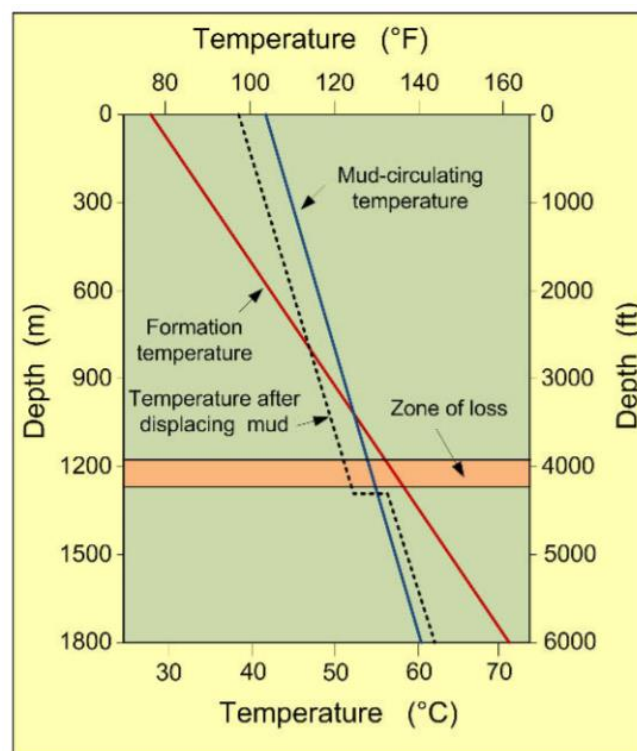


Figure 4.3: How lost circulation zones can be detected through temperature surveys; first, mud temperature is measured downhole after equilibrium with the formation is established. Then, fresh mud is circulated, and a new temperature measurement is done. From the black dotted graph (temperature of fresh mud), it is possible to see a sharp jump in temperature at the zone of loss (Gaurina-Medjimurec and Pasic, 2014).

It is also possible to say (not with 100% certainty, but a good indicator) if the loss zones are occurring near the drill bit or not by analysing the circumstances in which lost circulation occurred. If they were noticed while:

- Drilling ahead
- There was a change in ROP, torque or vibration
- Entering a vugular, fractured or high-permeability zone known from available geological data

it is believed that the losses occurred at the drill bit. However, if they were noticed while:

- Tripping in/out
- Increasing mud weight
- The well was shut-in or killed

there are reasons to believe that the losses occurred other places (Lavrov, 2016a).

However, when lost circulation has already occurred, there exists several techniques used for controlling the situation. They are all designed to seal off loss zones, and include (Mitchell and Miska, 2010):

- Remove the conditions that caused lost circulation, so the formation can heal itself.
- Use LCM (lost circulation material) or cuttings to bridge off loss interval (see Figure 4.4).
- Spot a high-viscosity plug over the loss interval (see Figure 4.5).
- Squeeze the loss interval with cement.
- Set casing/pipe across the loss interval.
- Abandon or sidetrack away from the loss interval.

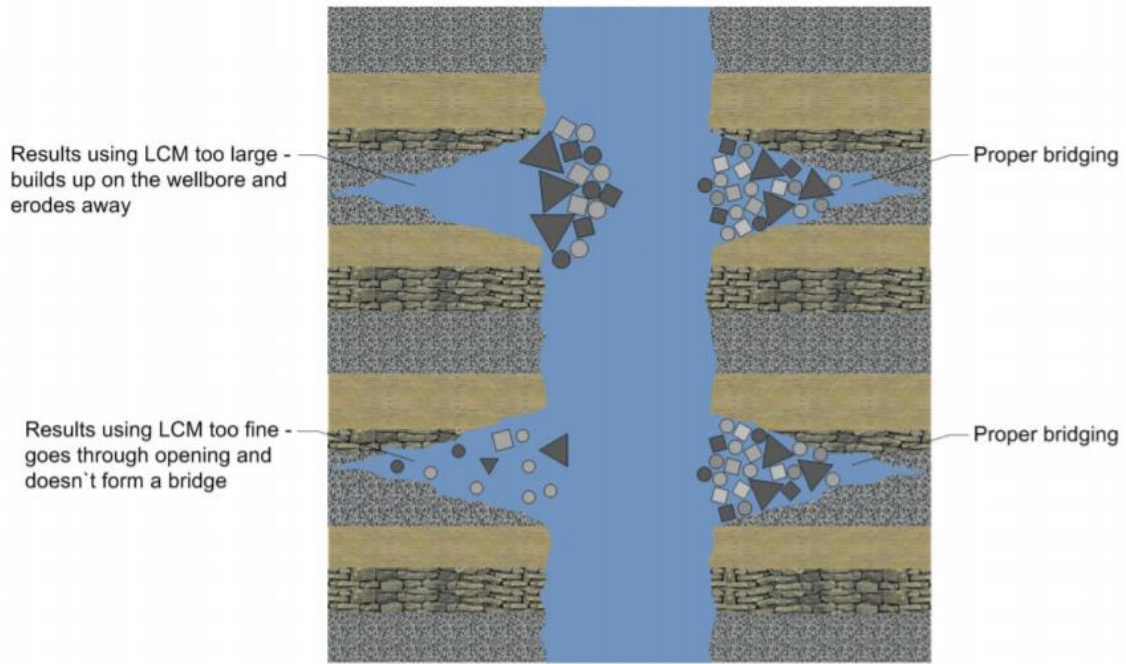


Figure 4.4: Improper fracture bridging can be seen on the left side of the hole, and proper fracture bridging to the right. This illustrates the importance of choosing the correct granular/fibrous/flaked sizes of LCM (Gaurina-Medjimurec and Pasic, 2014).

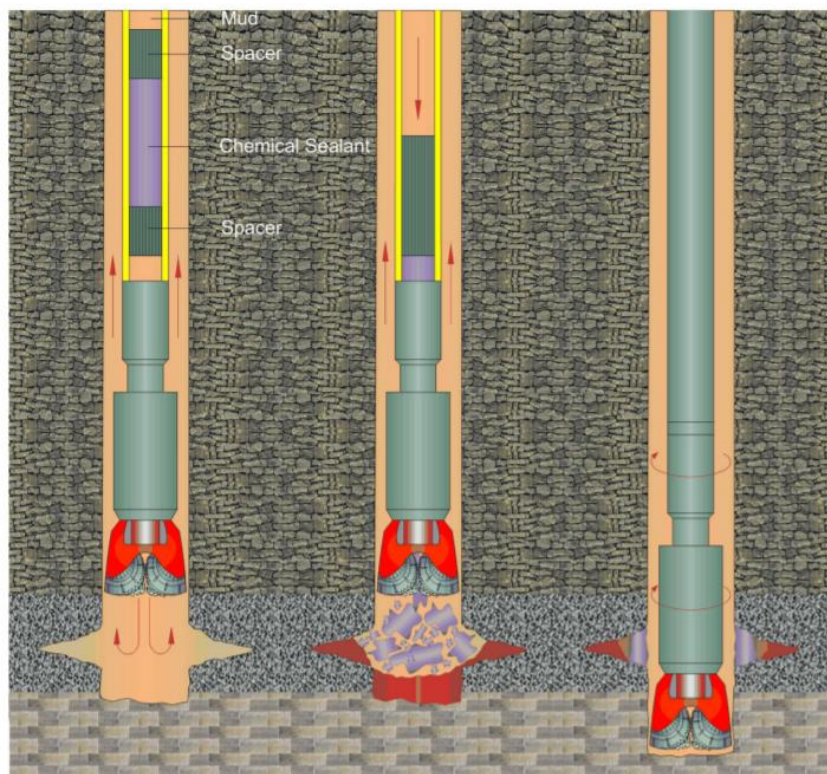


Figure 4.5: Operational procedure of chemical sealant placement. The mechanism is similar for setting plugs/pills. The drillstring is lowered to the loss area, where the pill is pumped into the formation or the chemical sealant is activated (Gaurina-Medjimurec and Pasic, 2014).

5. Model of mud pit volume

The main objective of this master thesis was to make a theoretical model of the mud tank volume during drilling operations. By comparing the theoretical model to observed data from the RTDD, it will be possible to test the accuracy of the model. In present master thesis, RTDD from well NO 1A (Statfjord C) was used. That well came with a final well report, which contained important information for making an accurate model. The theoretical model should detect unstable volume incidents in terms of unexpected volume level increase, or decrease. This chapter first introduces the basic concepts of the model, before parameters are described in more detail, and lastly the assumptions behind it:

5.1 Basic concept behind model

The mathematical model is expressed through the parameters affecting the tank level of the mud pit. By using mass conservation, and Figure 5.1 as a graphical representation of the situation, the basic model equation yields:

$$V_{in} - V_{out} = \Delta V_{pit} \quad (5.1)$$

Here V_{in} represents the volume changes that increase the mud pit volume, and V_{out} those that decrease it. The sum expresses the volume changes inside the mud pit, ΔV_{pit} . The elements that affect the mud pit level are:

$$V_{in} = V_{steel\ in} + V_{pump\ off} + V_{adj_up} \quad (5.1.1)$$

$$V_{out} = V_{steel\ out} + V_{cuttings+film} + V_{pump\ on} + V_{adj_down} \quad (5.1.2)$$

All parameters are defined in the Nomenclature chapter, and some from Figure 5.1.

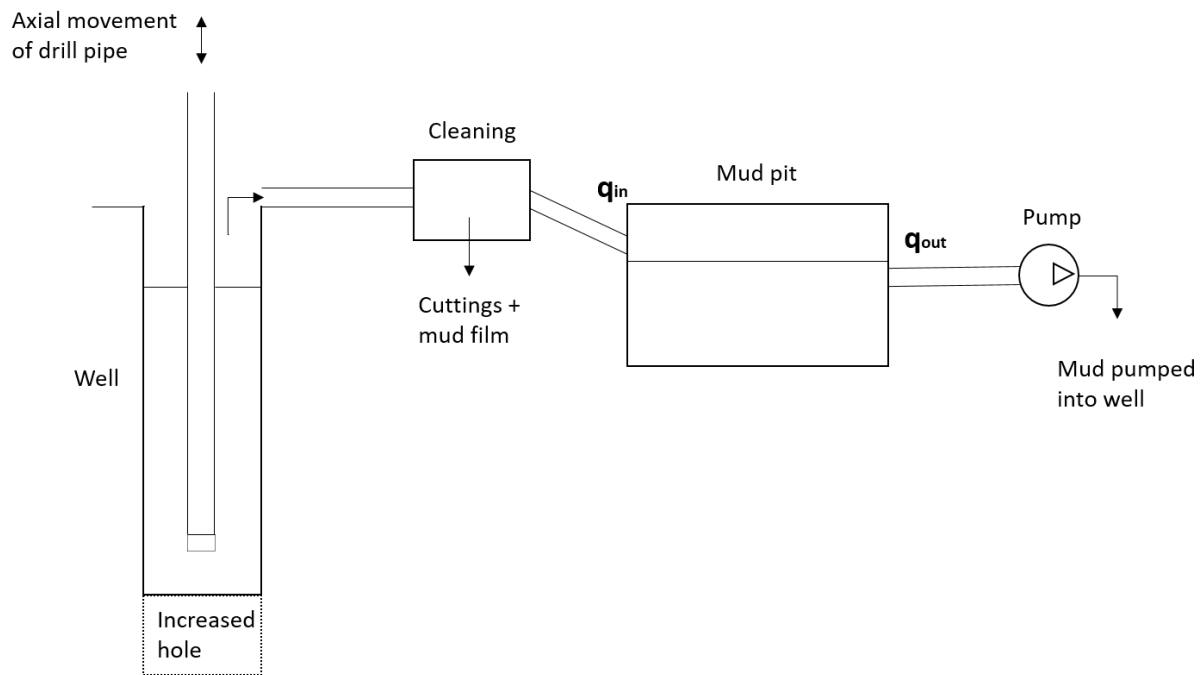


Figure 5.1: Overview of the mud circulation system, and the parameters that affect the mud pit level.

Equations 5.1.1 and 5.1.2 consider all the different elements that affect the fluid level inside the mud pit. Every component in the circuit (see Figure 5.1) causes changes of the pit level:

- Generation of cuttings from the hole
- Drillstring movement
- Mud lost with cuttings in the cleaning process
- Emptying/filling of surface lines when the pump is shut down/turned on.

The equation must include terms of flow rate and other RTDD-parameters. In this way, the model can be tested against the data collected from Diskos. When applying the RTDD-parameters, the equation expresses rates instead of volumes. The relation between flow rate, time and volumes is given in eqn. 5.2:

$$\int q_i * dt = V \quad (5.2)$$

When taken over intervals of constant flowrate, q , the following is obtained:

$$q * \Delta t = V \quad (5.2.1)$$

or:

$$q = \frac{V}{\Delta t} \quad (5.2.2)$$

Where: V = volume in time intervals of constant q.

In terms of RTDD-parameters, the components of eqns. 5.1.1 and 5.1.2 can be written as:

$$V_{\text{steel in/out}} = Cap_{DP} * (DBTM_t - DBTM_{t-1})$$

$$V_{\text{pump on/off}} = \left[V_{\text{max}} * \frac{q_p}{q_{p,\text{max}}} \right] (t)$$

$$V_{\text{cuttings+film}} = (DMEA_{\text{tlag}} - DMEA_{\text{tlag-1}}) * A_{\text{bit}} * K_{\text{film}}$$

$$V_{\text{adj}} = V_{\text{adj}}(t)$$

When inserting these terms into eqn. 5.1, and considering the mud pit volume with respect to time, the final, mathematical equation of the model is obtained:

$$Cap_{DP} * (DBTM_t - DBTM_{t-1}) - A * K_{\text{film}} * (DMEA_{\text{tlag}} - DMEA_{\text{tlag-1}}) + \left[V_{\text{max}} * \frac{q_p}{q_{p,\text{max}}} \right] (t) + V_{\text{adj}}(t) = V_{\text{pit}}(t) \quad (5.3)$$

As can be noticed from eqn. 5.1, this is the continuity equation applied on a control volume surrounding the mud pit (see Figure 5.2). The mass streams going into the control volume are positive, and the ones going out are negative. This equals the mass change in the mud tank over a certain time period:

$$\sum \dot{m}_{\text{in}} - \sum \dot{m}_{\text{out}} = \frac{dM_{\text{pit}}}{dt} \quad (5.4)$$

Here \dot{m} = Mass stream either in or out of the control volume, which can be written in terms of density (ρ), and flowrate (q):

$$\dot{m} = \frac{dm}{dt} = \frac{\Delta \rho V}{\Delta t} = \rho * \frac{\Delta V}{\Delta t} = \rho * q$$

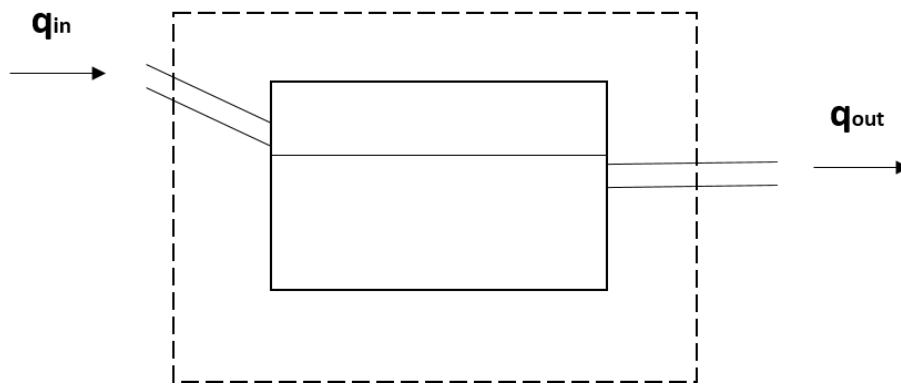


Figure 5.2: Control volume of the mud pit showing mass flow in and mass flow out.

The terms of equation 5.3 containing DBTM and DMEA, can be calculated directly from the RTDD-parameters as soon as the lag time, t_{lag} , is found and the capacity/size of the drill pipe is given. The other terms need to be found practically by evaluating the RTDD, and finding gradients, maximum values and other properties. In addition, several of the elements in the equation are not always valid. For instance, there will not always be performed adjustments, so the term $V_{adj}(t)$ is sometimes zero. More detailed information about the elements in the model and their belonging parameters is given in the following subchapter.

5.2 Parameters

This sub-chapter presents more detailed information about the terms and parameters of the model (see eqns. 5.1 and 5.3), and how they were obtained. The assumptions behind them are summarized in the end of each section.

5.2.1 V_{pit}

The term on the right side of eqn. 5.3, $V_{pit}(t)$, describes the mud pit level over time and is the final output of the model. When all necessary parameters have been obtained, the modelled TVA-volume can be found. An overview of the calculations is found in Table 5.1:

Table 5.1: *Some of the most important parameters and calculations of the theoretical model.*

DATE	TIME	DMEA	DBTM	MFI	DP mud displacement (5")	Adjustment	Vmax- [Vmax*(qp/qp_max)]	V_cuttings+ film	Real TVA	Model TVA
dd-mmm-yy	hh:mm:ss	M	M	M3/min	M3	M3	M3	M3	M3	M3
08.feb.06	10:30:00	7861.46	7861.46	1.51	0.00018	0	0.41	0.0014	128.41	133.48
08.feb.06	10:30:05	7861.48	7861.48	1.51	0.00019	0	0.41	0.0011	128.29	133.48
08.feb.06	10:30:10	7861.50	7861.50	1.51	0.00014	0	0.41	0.0014	128.11	133.48
08.feb.06	10:30:15	7861.53	7861.52	1.51	0.00019	0	0.41	0.0014	128.25	133.48
08.feb.06	10:30:20	7861.55	7861.54	1.51	0.00017	0	0.41	0.0012	128.33	133.47
08.feb.06	10:30:25	7861.57	7861.56	1.51	0.00017	0	0.41	0.0012	128.23	133.47

Figure 5.3 presents the real TVA measurements from well 1A together with model output:

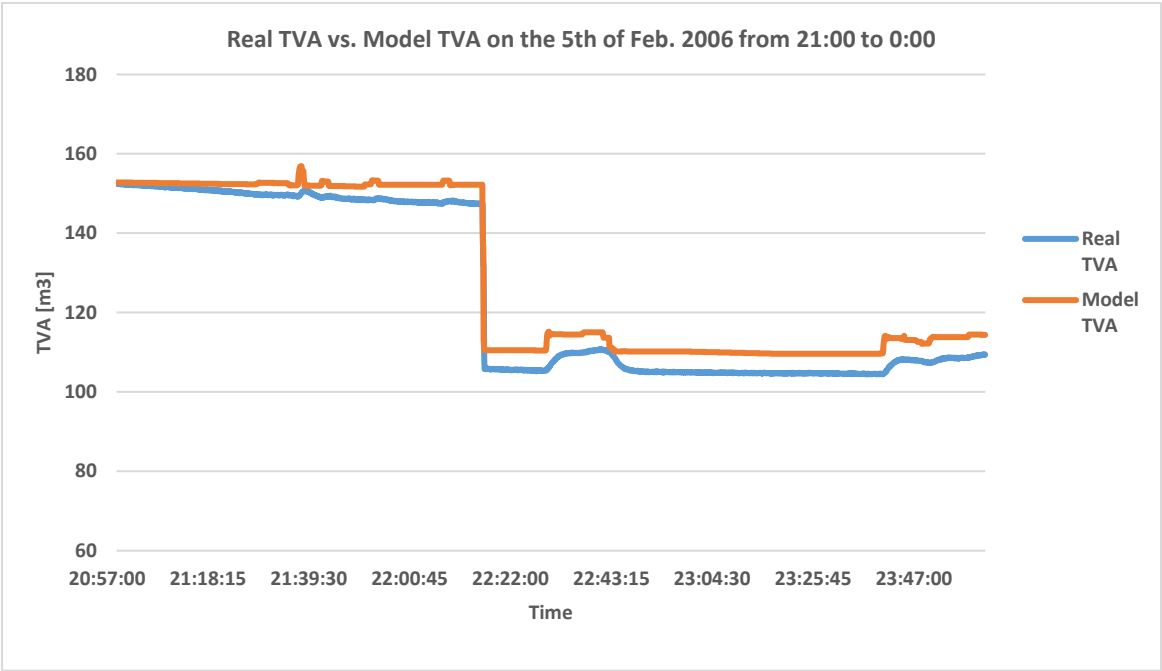


Figure 5.3: Real TVA measurements versus modelled values. From well 1A on the 5th of February 2006 from 21:00 to 0:00.

5.2.2 V_{in} and V_{out}

Each time drill pipe is either lowered or removed from the well, it will affect the volume level inside the mud pit. When steel is lowered into the well, the excess mud will cause an increase inside the tank, and the opposite when steel is removed. In most well reports, it is possible to find information about the drill pipe used. However, for well 1A, only drill pipe OD and ID were given -not the steel capacity. It was therefore necessary to look up this parameter in a separate drilling handbook, where detailed information on all drill pipe sizes can be found (see Appendix C for details).

In our theoretical model, this is obtained from bit depth (DBTM) gathered from the RTDD. Since these parameters are time based, the model needs to detect when drillstring movements are happening, and the distance it is moved at a certain time step. Because the RTDD are given with a time interval of five seconds, each time step of the model was set with an interval of five seconds as well. Table 5.2 shows the results of the calculations:

Table 5.2: *Steel displacement calculations for moving drill pipe.*

X-area 5" DP	0.008	m ²
--------------	-------	----------------

DATE	TIME	DMEA	DBTM	DP mud displacement (5")
dd-mmm-yy	hh:mm:ss	M	M	M ³
08.feb.06	6:00:05	7828.39	7828.39	0.00014
08.feb.06	6:00:10	7828.41	7828.40	0.00011
08.feb.06	6:00:15	7828.42	7828.42	0.00014
08.feb.06	6:00:20	7828.43	7828.43	0.00010
08.feb.06	6:00:25	7828.46	7828.45	0.00015
08.feb.06	6:00:30	7828.47	7828.47	0.00012

Table 5.2 shows a short glimpse of a drilling operation. It lasts for 30 seconds, and was performed on the 8th of February, 2006. The table contains information on the hole depth (DMEA), bit depth (DBTM), cross-section area of the drill pipe (with OD = 5" and ID = 3") and the mud displacement that is caused by lowering of the drill string each fifth second. As can

be seen, between 0,1 and 0,15 litres is gained in the TVA each time step, which corresponds to 1-2 cm of drill pipe. The volume displacement was calculated by this part of eqn. 5.3:

$$V_{\text{steel,in}} = Cap_{DP} * (DBTM_t - DBTM_{t-1}) \quad (5.5)$$

The same equation is also used when calculating the amount of steel that is pulled out of the well. The only difference is that the volume will be negative, indicating a decrease of the total TVA volume.

Assumptions

1. Volume changes due to steel, either lowered into or pulled from the hole, is detected immediately by the active mud tank.
2. The cross-sectional area of the drill pipe used for calculating steel volume displacement, was based on a drill pipe with OD equal to 5" and ID equal to 3", since no detailed information on exact drill pipe configuration was given.
3. For quick movements, closed-end drill pipe is assumed. For slow movements, it is assumed that the mud flows into/out of the pipe; i.e. open-end.

5.2.3 $V_{\text{cuttings} + \text{film}}$

During the cleaning process at surface, cuttings are removed from the mud system over the shale shaker. This affects the material balance in that more mud is eventually needed to account for the lost volumes. The cuttings originate from the bottom of the hole, and the amount taken out at surface in the mud cleaning system corresponds to the drilled size of the hole. The volume of cuttings that is lost at surface can therefore be calculated by considering the incremental hole growth volume:

$$(DMEA_{t_{\text{lag}}} - DMEA_{t_{\text{lag}}-1}) * A_{\text{bit}}$$

However, in addition one needs to account for mud that is sticking to the cuttings removed in the shaker. Wettability conditions dictate the cuttings to be water wet. Therefore, additional mud is lost with the cuttings as a mud film that cannot be cleaned. By adding a factor, K_{film} , to the hole-growth equation this can be accounted for:

$$(DMEA_{t_{\text{lag}}} - DMEA_{t_{\text{lag}}-1}) * A * K_{\text{film}}$$

The K_{film} factor needs to be found practically, and is unique for each well drilled. A typical value lays around 1,5.

Furthermore, for this term it is necessary to account for lag-time. At the moment when the cuttings are drilled downhole, no volume change is seen at the mud pit at surface. This level adjustment does not occur until the cuttings reach the shale shaker (see Figure 5.4). The time it takes for the cuttings to travel up from the bottom of the hole to surface is therefore equal to the lag-time, which has to be found and included in the calculations.

In order to find a good approximation for t_{lag} , the RTDD from well 1A was investigated. Since lag time is dependent on the flow rate into the well ($MFI = q_{\text{pump}}$) and the annulus volume throughout the well, it can be expressed by the following equation:

$$t_{\text{lag}} = \frac{V_{\text{ann}}}{q_p} \quad (5.6)$$

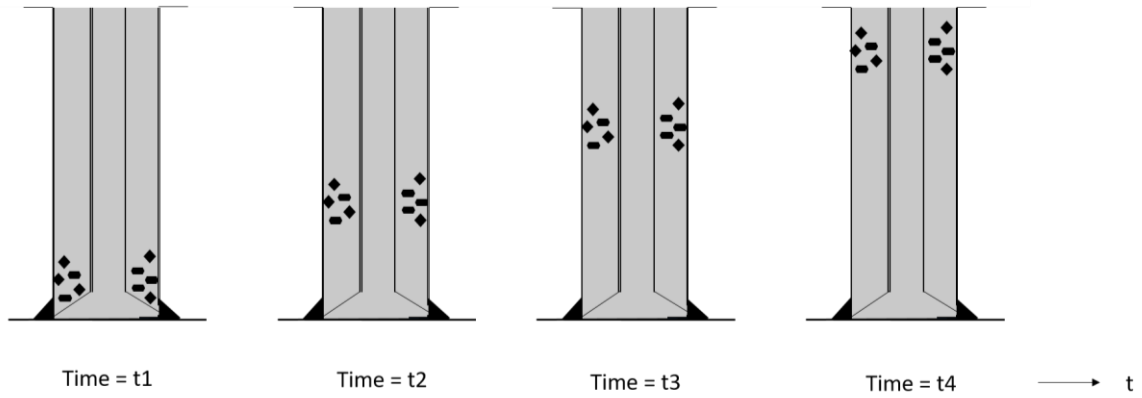


Figure 5.4: *The volume change caused by drilled cuttings will be felt at surface after a given “lag-time”.*

To simplify, it is assumed the average cuttings is transported at exactly the same velocity as the mud. However, because the flow rate changes throughout the drilling process, together with hole depth, some simplifications were done. By looking at the RTDD, it was possible to observe that the flow rate was quite stable at three different values throughout the operations in well 1A (see Figure 5.5).

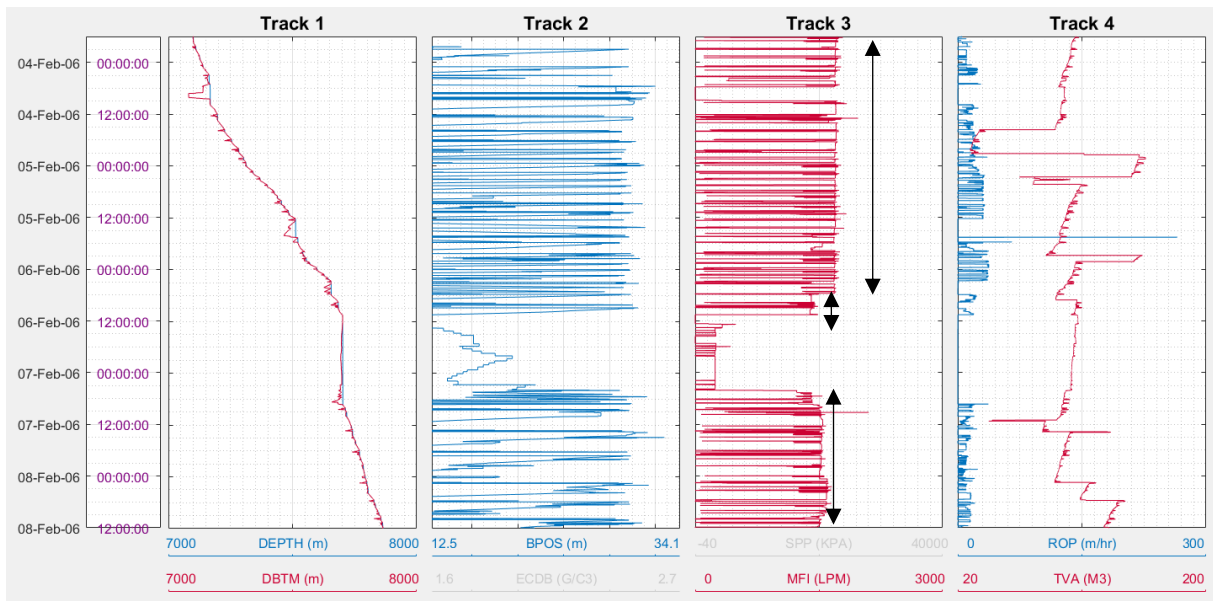


Figure 5.5: *Track 3 shows the flow rates from the mud pumps. As can be observed, it varies between three values during the drilling operations (indicated by the black arrows).*

The well was therefore separated into three sections based on the flow rate used within them. For each section, one average flow rate was found (all intervals where mud pumps were off, and the flow rate was zero, were excluded from the calculations). The results are presented in Table 5.3:

Table 5.3: Calculations of average pump flow rate in each section given in litres per minute.

	Average q_pump before 05:45, 6th of Feb. 2006	Average q_pump until 10:32, 6th of Feb. 2006	Average q_pump after 07.15, 7th of Feb. 2006
Equals interval [mMD]:	7099.57 - 7655.59	7655.59 - 7701.74	7701.74 - 7864.52
	[lpm]	[lpm]	[lpm]
	1530.70	1340.70	1439.33

Now, the annulus volume could be calculated for each time step, with the associated hole depth, for the separate sections. The average q_{pump} was then used to find lag-time at each depth. Lastly, an average lag-time was calculated for each section, that would be used for further calculations (see Table 5.4).

Table 5.4: Annular volume and lag-time calculations for period 1 with $q_{pump} = 1,53 \text{ m}^3/\text{min}$. Average lag-time for period marked in red.

Calculations for period 1:									
q-pump	Lag Depth	OH Length	Length of BHA in OH:	Length of BHA in Casing:	Length of DP in OH:	Length of DP in casing:	Annulus volume:	Lag time:	Average lag time for period:
[LPM] & [m3/min]	[mMD]	[mMD]	[mMD]	[mMD]	[mMD]	[mMD]	m3	[min]	[min]
1530.70	7100	30	30	97.52	0	6972.48	171.10	111.78	116
1.53	7110	40	40	87.52	0	6982.48	171.38	111.96	
	7120	50	50	77.52	0	6992.48	171.67	112.15	
	7130	60	60	67.52	0	7002.48	171.95	112.33	
	7140	70	70	57.52	0	7012.48	172.23	112.52	
	7150	80	80	47.52	0	7022.48	172.52	112.71	
	7160	90	90	37.52	0	7032.48	172.80	112.89	

Similar tables were made for all three sections, and the results were:

Table 5.5: Lag-time for all three periods.

	Period 1:	Period 2:	Period 3:
Depth [mMD]:	7099.57 - 7655.59	7655.59 - 7701.74	7701.74 - 7864.52
Lag time [min]:	117	140	132

When all lag-times were calculated, the real TVA measurements could be plotted against the modelled TVA. By doing so, the theoretical TVA model could be compared to the real measurements, and the amount of mud that disappeared from the system as a “film” covering the cuttings could be determined.

First, high quality investigation intervals were found from the RTDD. High quality intervals included areas where the real active tank level was decreasing at a steady rate, and the corresponding ROP was known, for a certain period. In total, five intervals were chosen (see Figure 5.6).

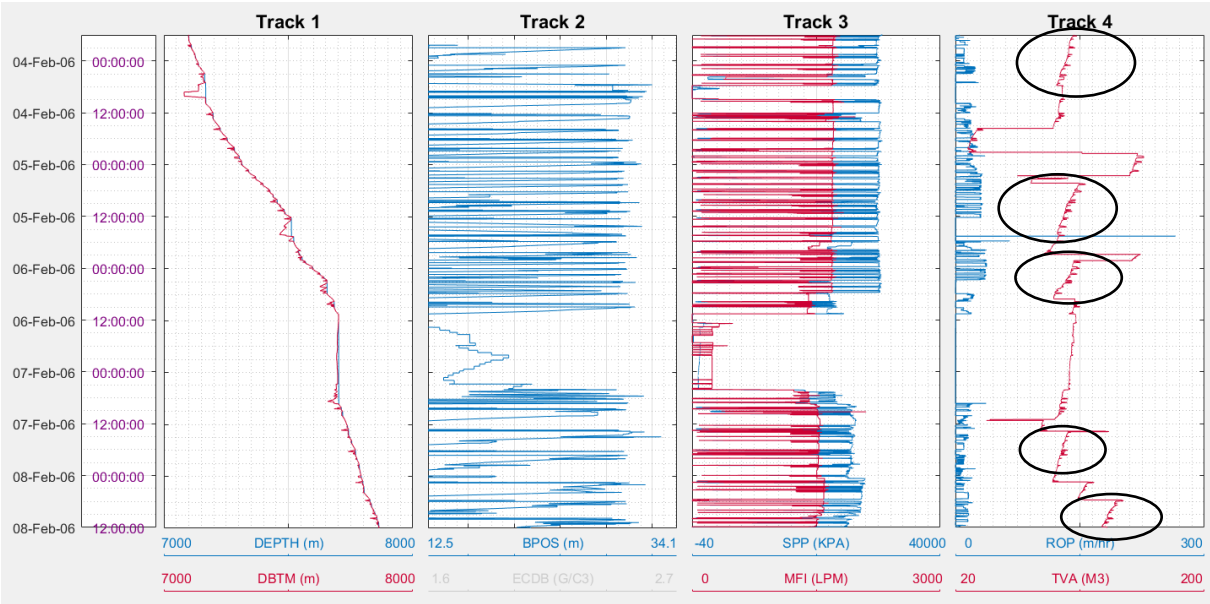


Figure 5.6: Five intervals were found out from the TVA measurements in track 4 (black circles).

Each interval was then evaluated stepwise. Date, time, hole depth (DMEA), bit depth (DBTM) and the real TVA-measurements were loaded into Excel from the original RTDD-file. By taking the lag-time into account, the theoretical volume change in the active mud pit could be calculated at each time step, as the bit diameter was known (8,5" x 9" section). The Excel spreadsheet was set up in the following way (3rd of February 2006):

Table 5.6: *Calculations of theoretical mud volume needed to fill drilled volume.*

DATE	TIME	DMEA	DBTM	Volume change at surface after lag-time for 8,5" hole	Volume change at surface after lag-time for 9" hole	DP mud displacement (5")
dd-mmm-yy	hh:mm:ss	M	M	M3	M3	M3
03.feb.06	19:57:05	7106.21	7106.20	0.00025	0.00028	0.00011
03.feb.06	19:57:10	7106.22	7106.22	0.00025	0.00028	0.00012
03.feb.06	19:57:15	7106.23	7106.23	0.00025	0.00028	0.00014
03.feb.06	19:57:20	7106.25	7106.25	0.00023	0.00026	0.00013
03.feb.06	19:57:25	7106.27	7106.27	0.00034	0.00038	0.00011
03.feb.06	19:57:30	7106.28	7106.28	0.00023	0.00026	0.00012

It is important to note that the volume change-columns take in incremental hole depth 117 minutes earlier -this because lag-time had to be included. The steel displacement calculations are, however, taken at the instant bit depths. It is also worth noticing that two volume changes have been calculated. This because it was difficult finding information about when and where (on the BHA/drillstring) the hole diameter was enlarged from 8,5" to 9". Two TVA-models were therefore plotted in order to see which model was most accurate.

In addition, ROP-data from the well was loaded into the spreadsheet so that the theoretical drilled volumes could be calculated twice, and double-checked by two different methods. It was confirmed that the theoretical drilled volume was approximately 0,0003 m³/5s in both cases (see Table 5.7). From ROP, this is found by multiplying with A_{bit}:

$$q_{hole} = ROP * A_{bit} \tag{5.7}$$

Table 5.7: Based on ROP, the hole volume drilled was calculated together with cuttings concentration at the bottom of the well.

Rate of Penetration m/hr	Rate of Penetration m/5s	ROP*A (8,5) m3/5s	ROP*A (9) m3/5s	Concentration of cuttings at bottom, C (8,5)	Concentration of cuttings at bottom, C (9)
4.8	0.0067	0.00025	0.00028	0.0019	0.0022
5.1	0.0071	0.00026	0.00029	0.0020	0.0023
5.1	0.0071	0.00026	0.00029	0.0020	0.0023
5.1	0.0071	0.00026	0.00029	0.0020	0.0023

Two different theoretical TVA-models were now obtained; one based on a hole diameter of 8,5" and one of 9". They considered volume decreases in the mud pit because of increased hole size drilled and increases in mud pit level caused by additional steel lowered in the well. However, it was easy to observe that the 9" TVA model was the most correct one. K_{film} could now be found by comparing the slopes of the two graphs in each of the five intervals:

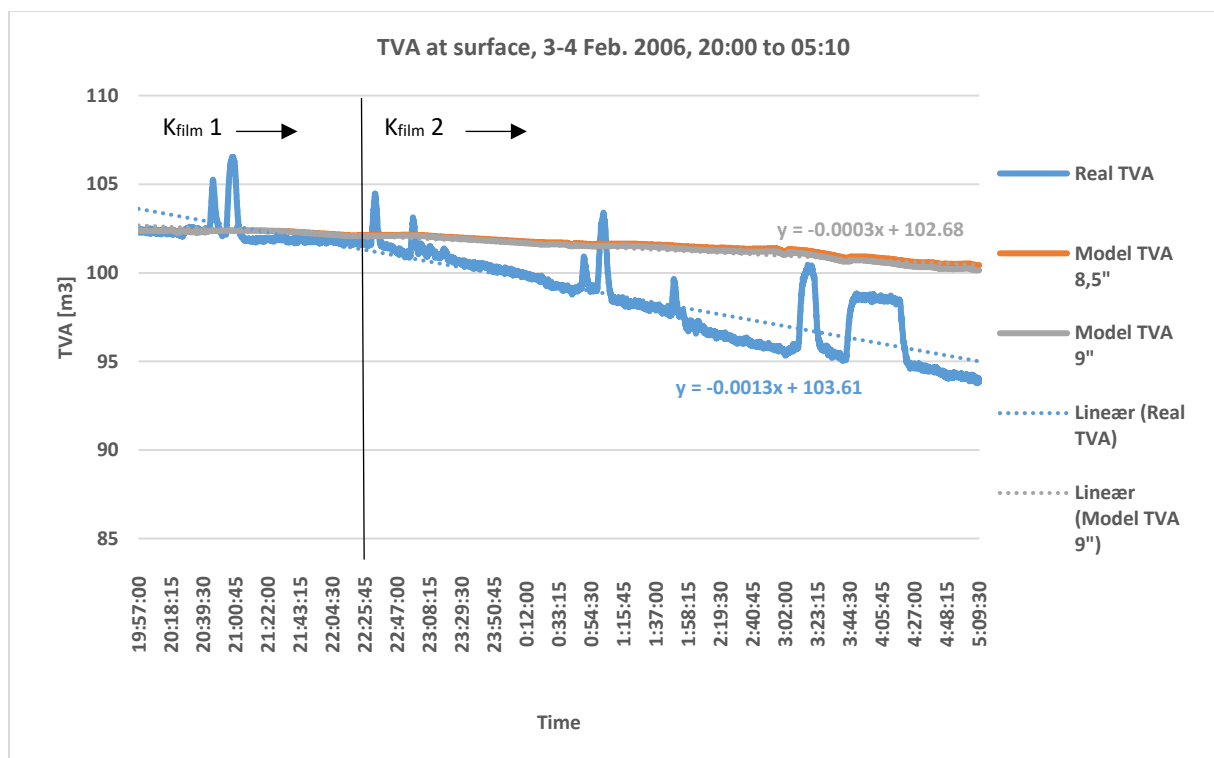


Figure 5.7: The real TVA measurements vs. the modelled one for a 9" hole. From 3rd - 4th of February 2006, 20:00 to 05:10. Two different K_{film} -values were found for making results more accurate.

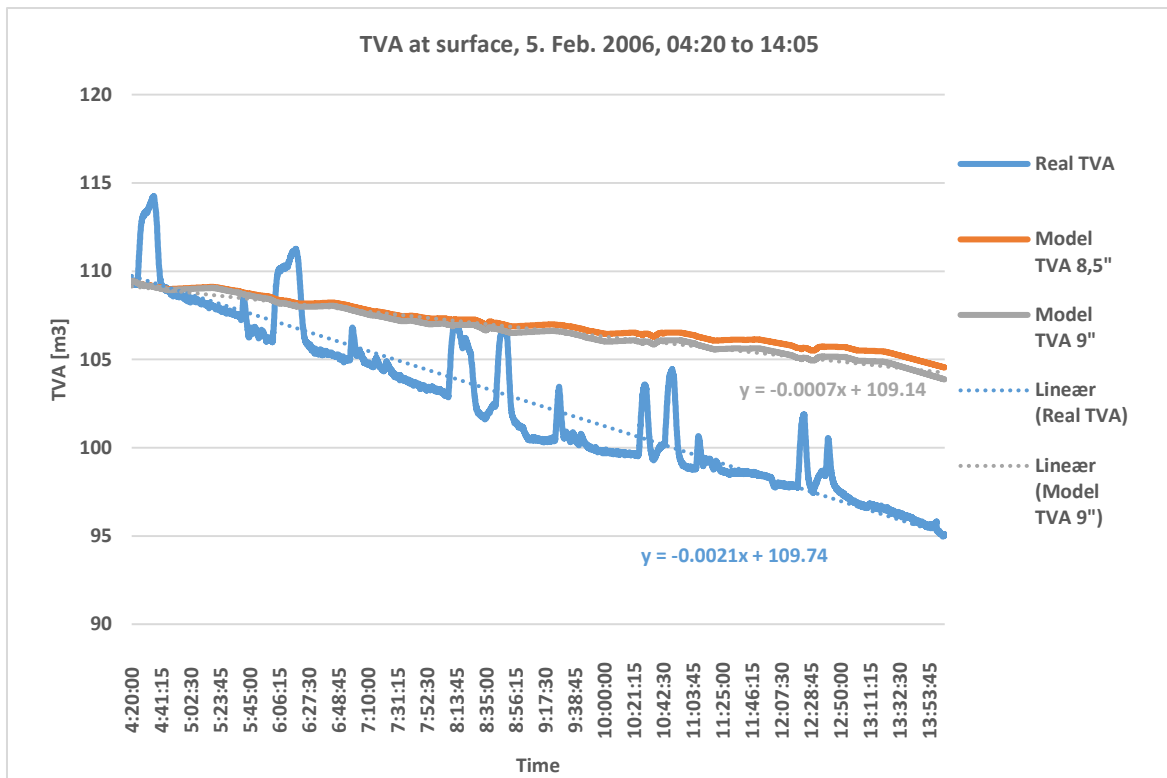


Figure 5.8: The real TVA measurements vs. the modelled one for a 9" hole. From the 5th of February 2006, 04:20 to 14:05.

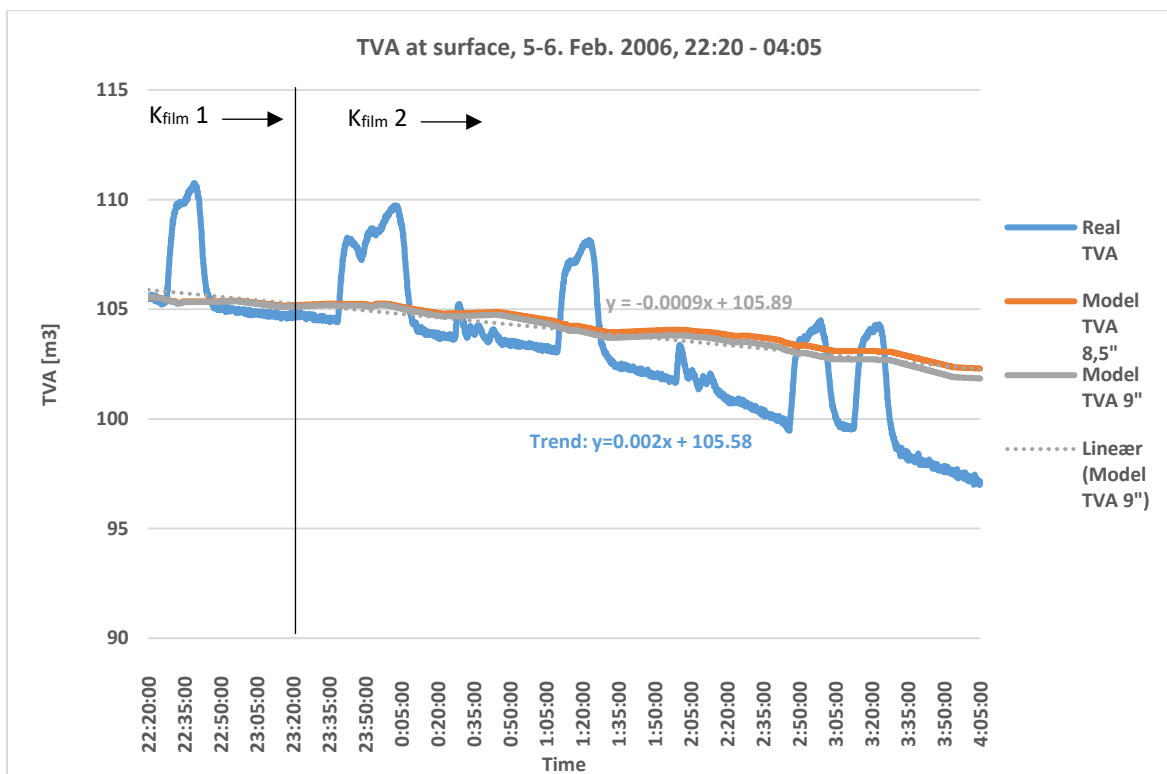


Figure 5.9: The real TVA measurements vs. the modelled one for a 9" hole. From the 5th – 6th of February 2006, 22:20 to 04:05.

The “jumps” seen on the real TVA-graph in Figure 5.9 represent flowbacks/flow-ins from the surface lines, as the mud pumps are shut off. In this interval, they interrupt the trendline slope that is made automatically in Excel quite heavily. The slope line was therefore calculated manually instead, by finding the first and last value of the true TVA data, and divide them by the amount of measurements:

$$\frac{\Delta y}{\Delta x} = \frac{(105,581 - 97,079)}{4141} = 0,002$$

The trend line equation therefore becomes $y = 0,002x + 105,58$, as written in the graph. This gives a $K_{film(2)}$ value equal to 2,2.

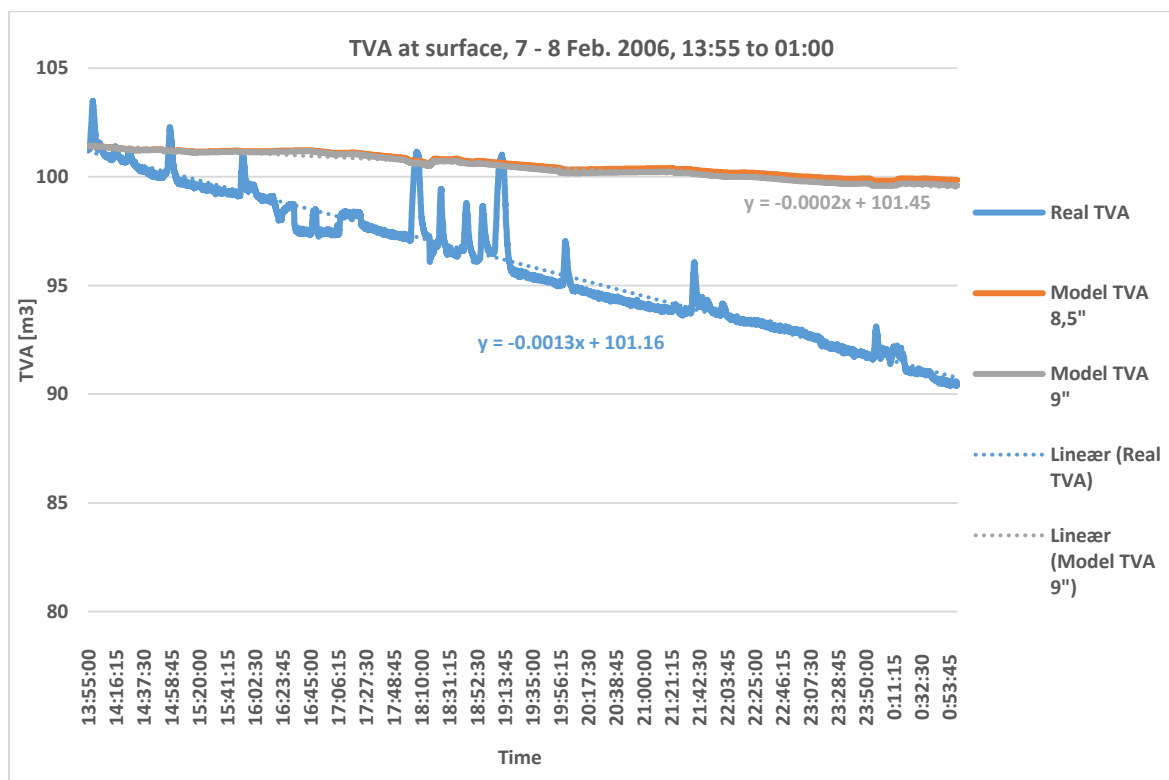


Figure 5.10: The real TVA measurements vs. the modelled one for a 9” hole. From the 7th – 8th of February 2006, 13:55 to 01:00.

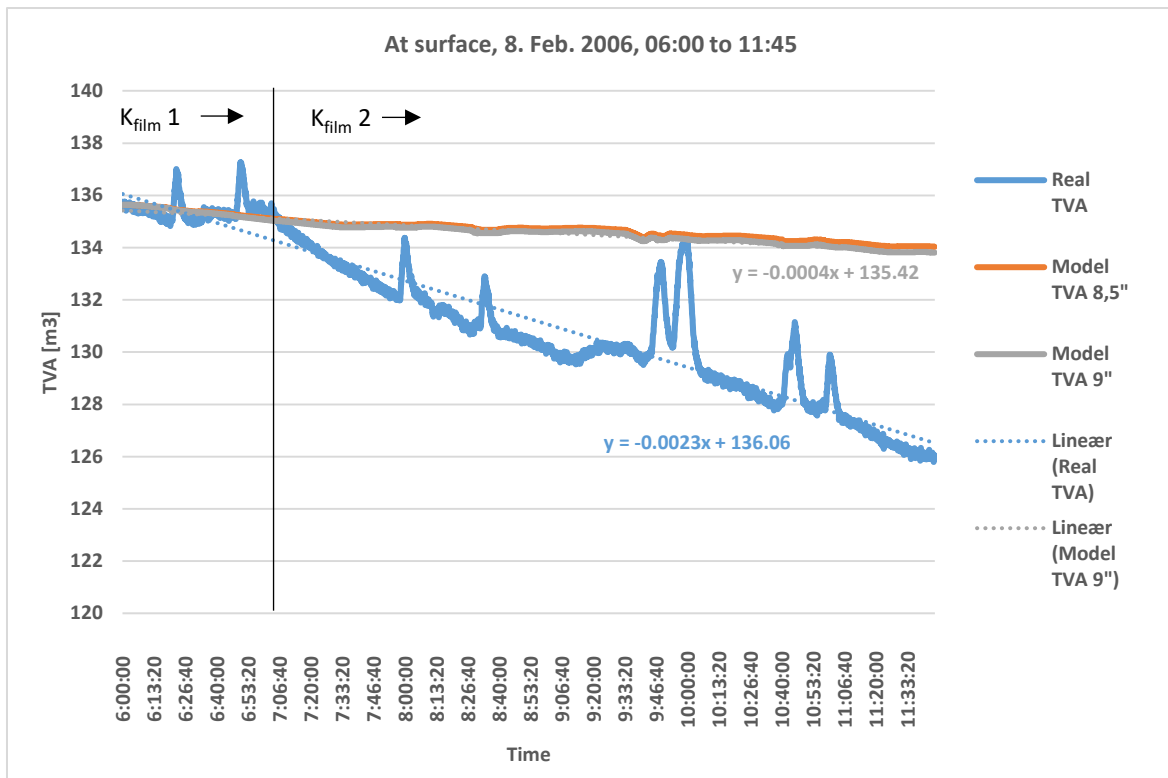


Figure 5.11: The real TVA measurements vs. the modelled one for a 9" hole. From the 8th of February 2006, 06:00 to 11:45.

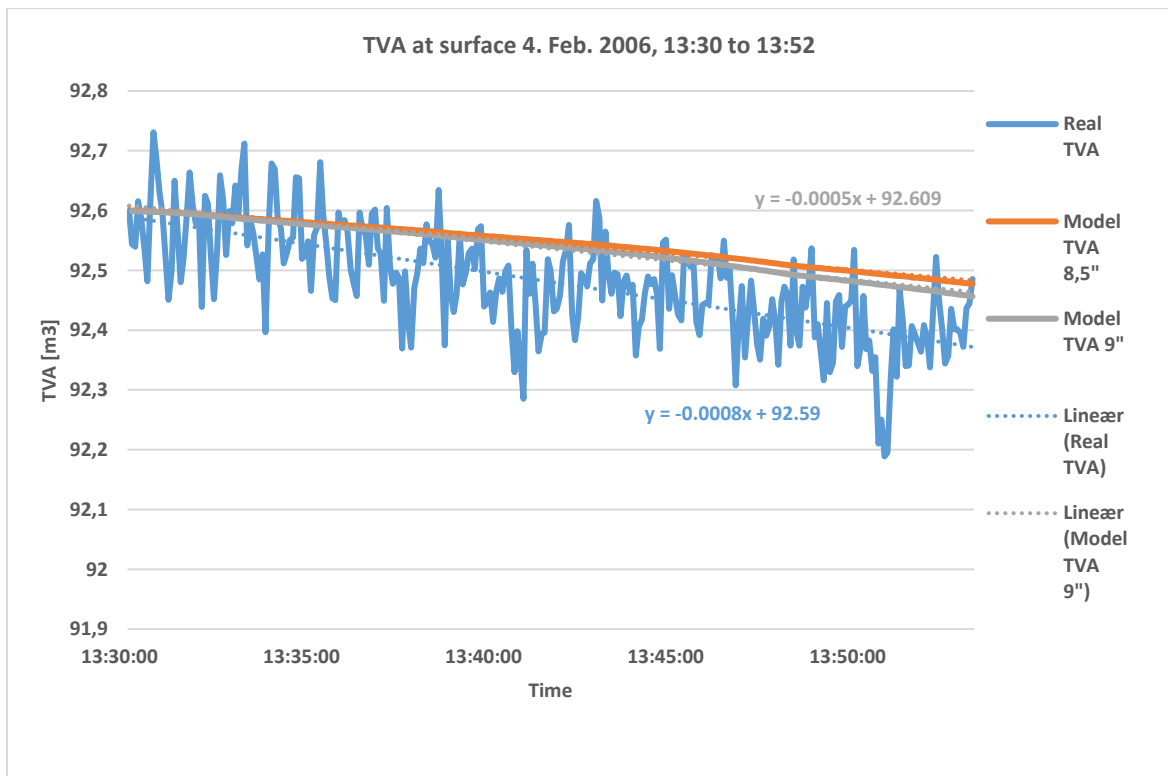


Figure 5.12: The real TVA measurements vs. the modelled one for a 9" hole. From the 4th of February 2006, 13:30 to 13:52.

Figure 5.12 represents another interval where the two graphs are quite similar, and a K_{film} could easily be calculated. In this case K_{film} was equal to 1,6.

When all intervals had been investigated, and different K_{film} -values were found, the results were organized in Table 5.8, and a final K_{film} was found by taking an average of the smaller values, which are more typical and correct values one could expect of K_{film} .

Table 5.8: Overview of K_{film} -values from the intervals investigated.

Start date	End date	Start time	End time	K_{film_1}	K_{film_2}
[dd.mm.yyyy]	[dd.mm.yyyy]	[hh:mm]	[hh:mm]		
03.02.2006	04.02.2006	20:00	05:10	1.53	4.3
04.02.2006	04.02.2006	13:30	13:52	1.6	
05.02.2006	05.02.2006	04:20	14:05		3
05.02.2006	06.02.2006	22:20	04:05	1.50	2.2
07.02.2006	08.02.2006	13:55	01:00		6.5
08.02.2006	08.02.2006	06:00	10:48	1.47	5.75
Average K_{film}				1.52	

The chosen value of K_{film} for the model was therefore:

$$K_{film} = 1,52$$

Assumptions

1. An average q_{pump} found for each section is used when calculating lag-time.
2. An average lag-time, t_{lag} , is used, even if hole depth continuously increases, and the real lag-time would have increased with depth.
3. During annular volume calculations, an average OD was assumed for the BHA. Average OD was 0,166 m.
4. The open-hole size was assumed to be 9".
5. Cuttings moved up through the well with the same velocity as the mud. Slip velocity was neglected.
6. It was assumed that 100% of the drilled cuttings reached surface.
7. Trend lines were used to give an acceptable approximation of the active tank levels when calculating K_{film} . When necessary, trend lines were calculated manually.
8. Assumed that 9 5/8" casing was hung off at RKB-level, and that the ID of this casing could be used for annular volume calculations up to the flow line (see Figure 5.13).

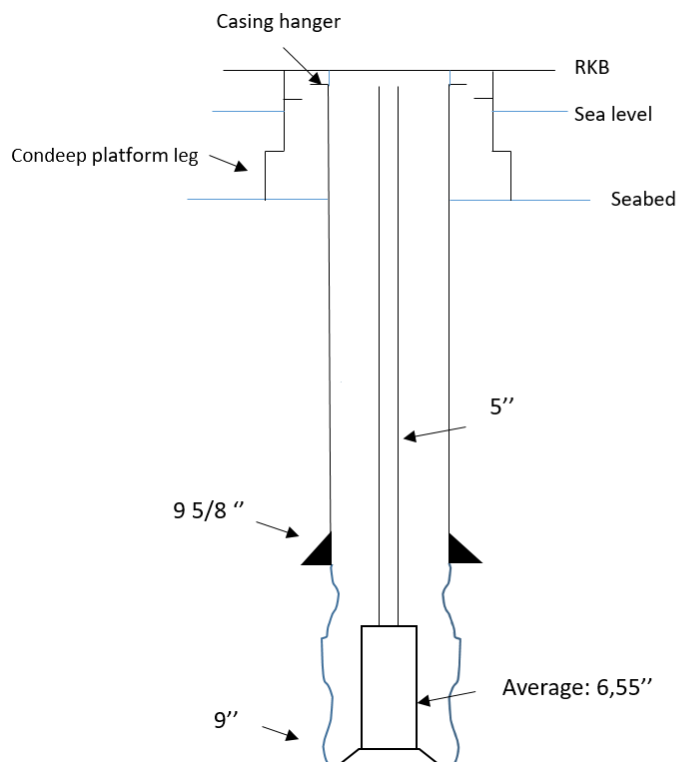


Figure 5.13: Overview of the condeep platform's well configuration.

5.2.4 Determining filling and emptying volume each time the pump is turned off/on (V_{pump})

Each time the pumps are turned on or off, the mud tank level is affected. Because of several open surface lines, mud can be stored there. When the mud pumps are turned off, the mud stored in the surface lines flows back into the mud pit. This causes a temporary increase of the mud pit level. Similarly, the same mud volume will be seen as decrease of the pit each time the pumps are started, because the empty surface lines are filled with mud.

How much mud that is stored in the surface lines can be found practically by investigating the volume influence on the mud pit each time the pumps are turned on or off. However, the pumps need to be shut down sufficiently long for the levels to stabilize (it takes time to empty a system completely). In this thesis, the pumps had to be shut down for 10 minutes or more, for the data to be used. In total, well 1A contained four periods with acceptable settling time, that were used for further calculations.

The four intervals were found by analysing the MFI-parameter (q_{pump}) from the RTDD in the log viewer. By going through every time step, one could distinguish the time intervals with the pumps shut off quite easily (see inserted box in Figure 5.14).

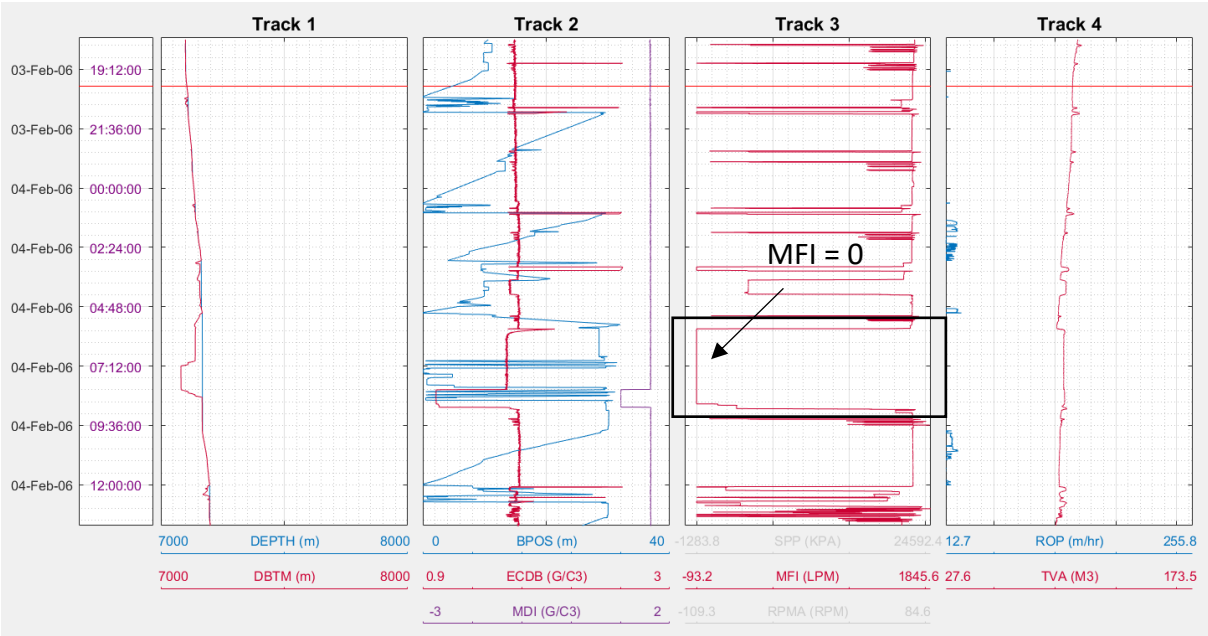


Figure 5.14: The pump flow rate is found in track 3. Observe that the pumps are shut down between 05:40 and 8:45 on the 4th of February 2006 (black box).

Each of the four pump intervals were then plotted in Excel together with the mud pit level vs. time. It was then possible to read the mud pit level changes with high accuracy at the moment the pumps were shut down and started again. The different graphs are presented below:

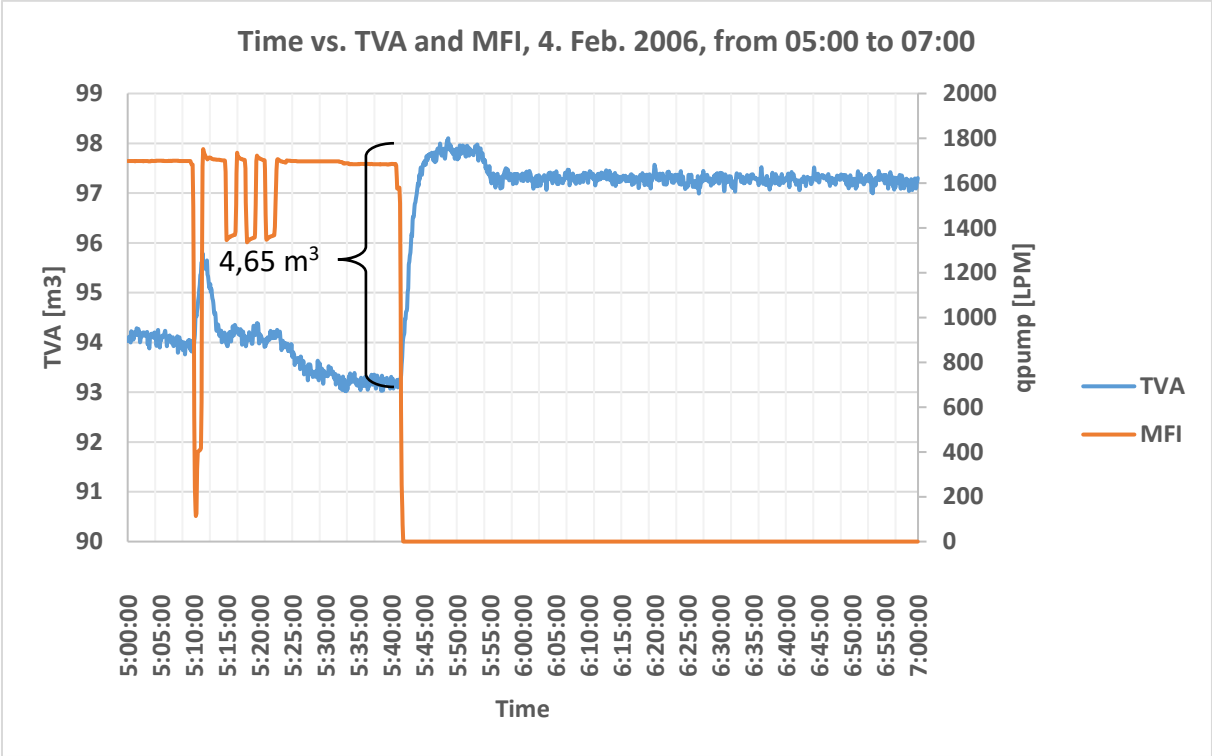


Figure 5.15: Time vs. TVA and MFI (q_{pump}) on the 4th of February from 05:00 to 07:00.

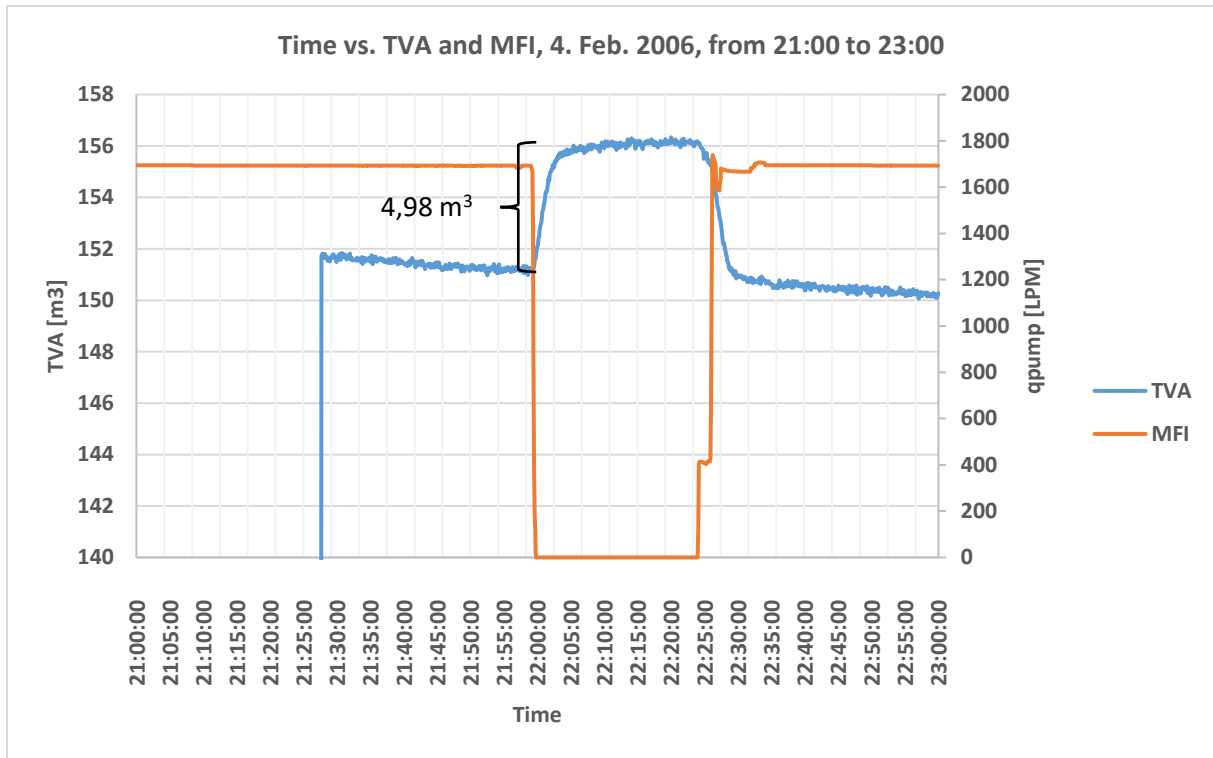


Figure 5.16: Time vs. TVA and MFI (q_{pump}) on the 4th of February from 21:00 to 23:00.

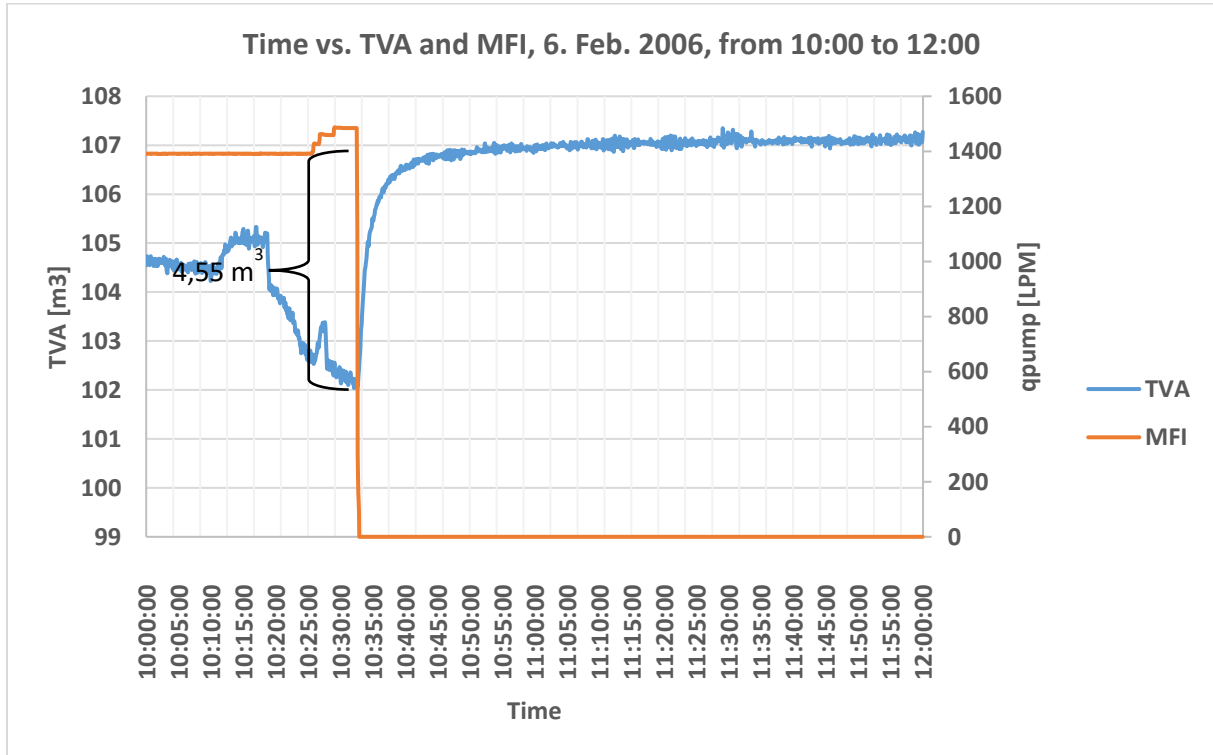


Figure 5.17: Time vs. TVA and MFI (q_{pump}) on the 6th of February from 10:00 to 12:00.

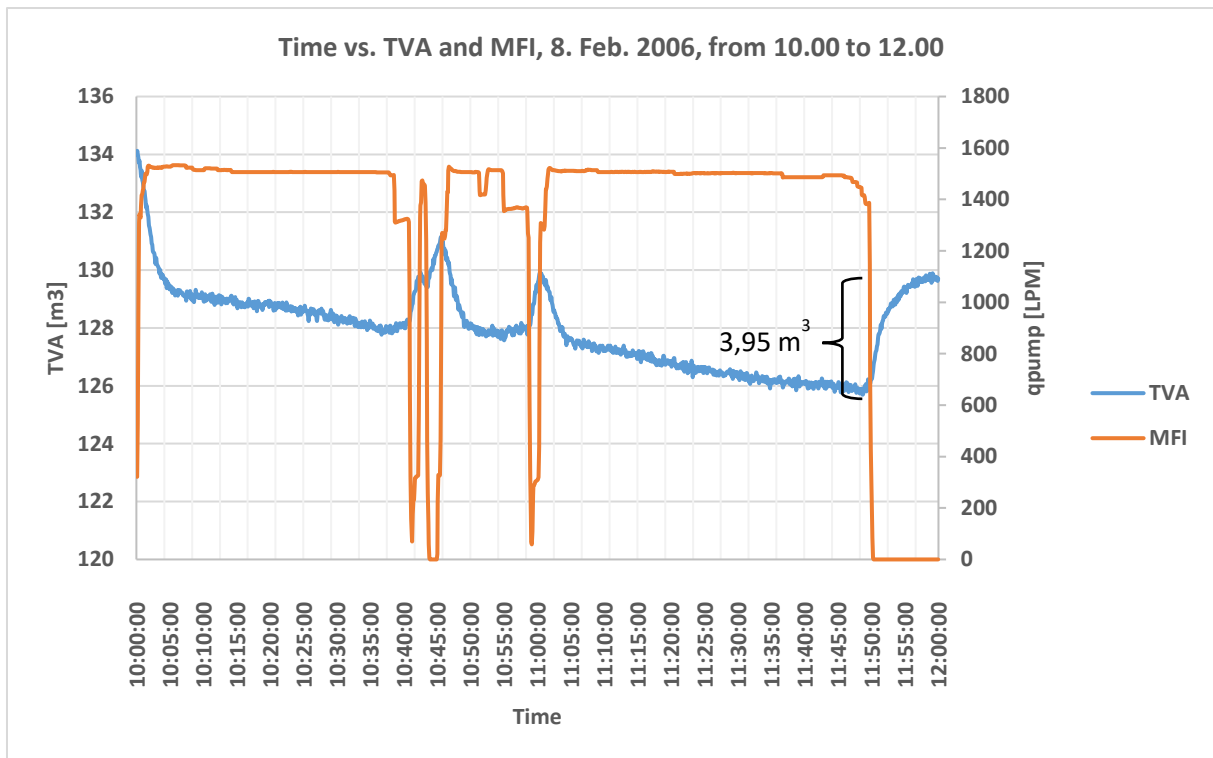


Figure 5.18: Time vs. TVA and MFI (q_{pump}) on the 8th of February from 10:00 to 12:00.

Figure 5.18 shows several time intervals where the mud pumps are either shut down, or pumping at low flow rates. It is however only the last pump shut-off that is useable, considering that the other periods do not have enough stabilization time for the fluid to flow back from the flowlines. In addition, the shut off should be as steep and clean as possible, with more stable flow rates, for the results to be accurate.

The mud pit level increases detected from the four time intervals were then organized into a table:

Table 5.9: Results of TVA level increase after pump shut-off.

Date	Start time	End time	qpump, before	qpump, before	qpump, after	TVA, before	TVA, after	Δ TVA
[dd.mm.yyyy]	[hh:mm]	[hh:mm]	[LPM]	[m3/min]	[LPM]	[m3]	[m3]	[m3]
04.02.2006	05:00	07:00	1685.17	1.69	0	93.20	97.85	4.65
04.02.2006	21:00	23:00	1692.78	1.69	0	151.20	156.18	4.98
06.02.2006	10:00	12:00	1484.83	1.48	0	102.15	106.70	4.55
08.02.2006	10:00	12:00	1493.70	1.49	0	125.80	129.75	3.95

And the results were plotted, in order to make a trend line that could be used for predicting the volume increase caused by flowbacks from the surface lines when flow rate, q , is given:

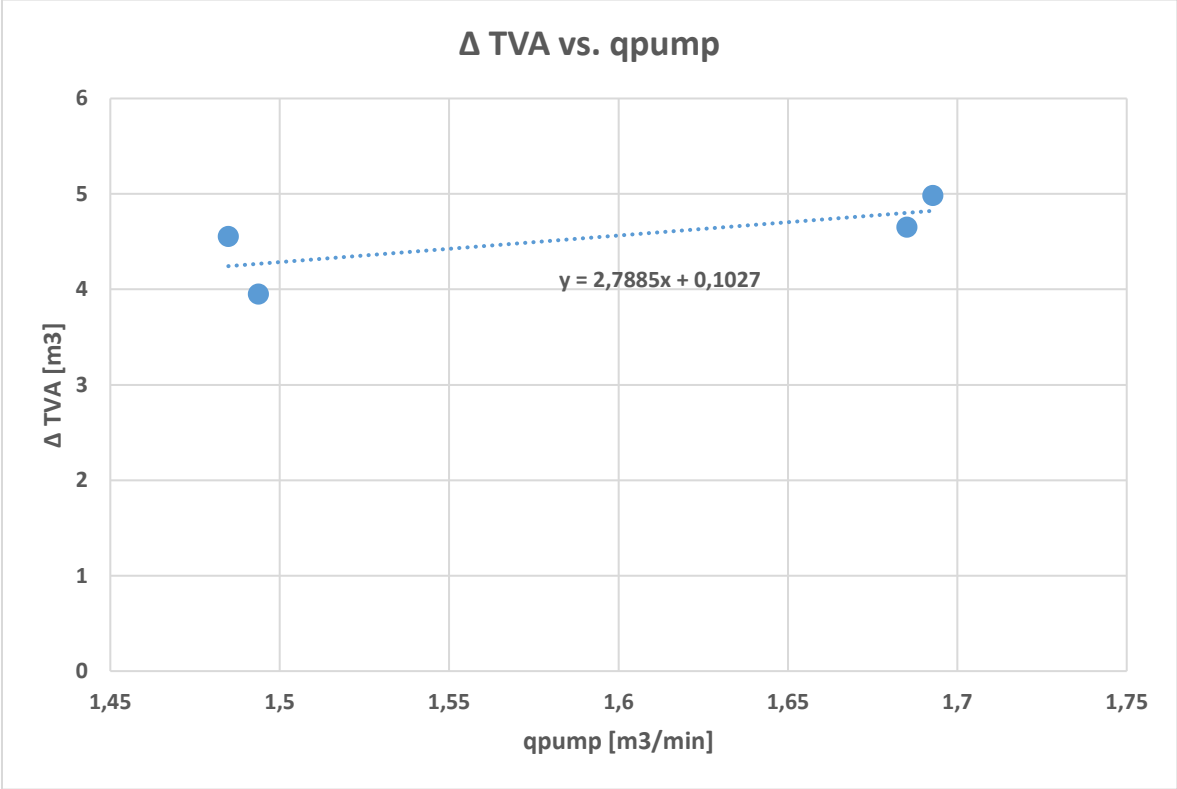


Figure 5.19: Trendline describing the relationship between volume stored in surface lines, ΔTVA , and pump flow rate, q .

The graph in Figure 5.19, and its belonging equation, can be used for finding a specific V_{max} based on maximum flow rate from the mud pump, $q_{pump, max}$. When V_{max} is found, it can be applied in the model (eqn. 5.3) and the volume gain in the TVA can be calculated at all times dependent on the flow rate, q_p .

Assumptions

1. Distance between mud pumps and mud tank was neglected. No lag-time was included.
2. The first measurement of volume level in mud tank was taken as the pumps were shut off. The last was taken approximately 10 minutes after pump shut-off.
3. The trend line used to describe the relationship between ΔTVA and q_{pump} was assumed to be linear (see Figure 5.19).
4. Fluid viscosity was assumed constant.

5.2.5 $V_{\text{adjustments}}$

During the drilling operation, several adjustments of the mud pit level are done. These adjustments can be observed as sudden jumps, or decreases, of the mud pit level (see track 4 from the RTDD in Figure 5.20). In the model, they are defined as $V_{\text{adj}}(t)$, and can be both positive or negative, dependent on which adjustment is being made.

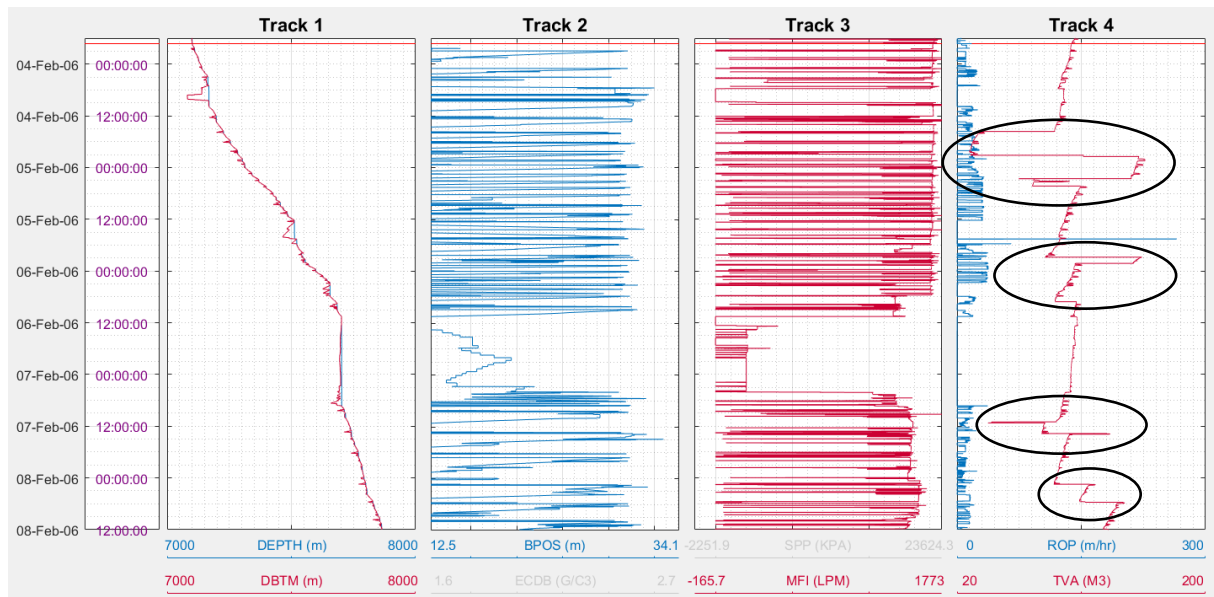


Figure 5.20: Track 4 shows the active tank volume (TVA), where several adjustments can be observed inside the black circles.

Throughout the operations in well 1A there are performed approximately 10 adjustments. They vary from small adjustments of 11,3 m³ to large adjustments of 81,54 m³. Common for all of them, is that the volume change is made immediately. In other words, they can be detected over one, or two time steps of five seconds. The cause behind these adjustments is the need for connecting or disconnecting the active mud pits on the rig. As can be seen in Figure 3.3, there exist several active tanks on a drilling rig. They can be connected and disconnected based on the volume needed for a specific operation, or for keeping the mud properties in acceptable condition for circulation.

The fact that each adjustment is performed immediately, makes it easy to implement in the model. Because all volume changes larger than 10 m³ are recognized as adjustments, every time step can be compared with the previous one for comparison. As soon as the difference is greater than 10 m³, the volume change is detected and added to the modelled TVA-volume.

In Excel, this was implemented by eqn. 5.8. It was then possible to find all time steps where the TVA level was either increased or decreased with more than 10 m³. The accurate volume change was then saved in a “cumulative adjustment volume”-column that was included in the model.

$$\begin{aligned}
 & \mathbf{if} \ (Real\ TVA_t - Real\ TVA_{t-1}) > 10 \ \mathbf{or} \ (Real\ TVA_t - Real\ TVA_{t-1}) < -10 \\
 & \quad \mathbf{then} \ Adjustment = (Real\ TVA_t - Real\ TVA_{t-1}) \\
 & \quad \mathbf{else} \ Adjustment = 0 \qquad \qquad \qquad (5.8)
 \end{aligned}$$

Assumptions

1. Absolute volume increases, or decreases, larger than 10 m³ were assumed to be adjustments.
2. The adjustments were assumed to be caused by switching, connecting or disconnecting of the active mud tanks.

6. Cases for testing model

The RTDD used in this master thesis is downloaded from Diskos, the Norwegian National Data Repository for Petroleum data. At the beginning of this master thesis (January 2017), NTNU was in possession of such a database. However, the database was very limited, with well data from 8 wells only. It was therefore necessary to increase the amount of such in-stock well data. Therefore, an introductory task of this master thesis has been to gather and clean data from Diskos. The additional files will then be used for more extensive testing of the model. This chapter considers in more detail how the well data was gathered, the databases involved and the cleaning process.

6.1 Existing database

The first version of the Drilldb\$-database only contained RTDD from 8 wells. End of well-reports for all 8 wells, were also available, and a log viewer was made for visualization and inspection purposes of the RTDD. The log viewer was designed and programmed by Anisa Noor Corina (Corina, 2017), and consists of one large, main script, and a template script that can be customized for specific log viewer modes, see Figure 6.1 (the full template script can be found in Appendix B).

```
1 % TRACKS TEMPLATE -- DO NOT CHANGE THE VARIABLE NAME
2 % For each curve track, it contains field:
3 % 1. Name = the name of the track preferred by the users
4 % 2. Curves = the curves assigned in each track
5 % 3. XScale = linear or logarithmic axes for the track
6 inputTrack = struct(...
7     'Name',      {'Track 1','Track 2','Track 3', 'Track 4'
8     },...
9     'Curves',   {{'DEPTH','DBTM'},...
10                {'BPOS','ECD','MDI'},...
11                {'WOB','TRQ'},...
12                {'SPP','ROP','TVA'}},...
13     'XScale',   {'linear','linear','linear','linear'});
14
```

Figure 6.1: An outcrop of the template script.

Figure 6.1 shows the template customized with parameters that are desirable when considering lost circulation cases. These variables can easily be changed for an influx situation, or any other failure that is to be investigated. The script contains good instructions and descriptions on how the set up should be, and an overview of all adjustments that can be done to optimize the interface. A list of shortcuts used for each RTDD-parameter can also be found in a separate file in the data base together with a user manual (Corina, 2017). The main script is located in the same database.

6.2 Diskos

The Diskos National Data Repository (NDR) is the national data repository for petroleum data in Norway. It is a joint venture that consists of the Norwegian Petroleum Directorate (NPD) and several oil companies on the Norwegian Continental Shelf. Diskos was established in 1995 to develop and operate a database containing relevant petroleum data, and its main tasks are reporting to authorities, trading and sharing of data between licensees and managing access to public data.

Oil companies operating in Norway need to share well data with the government (mandatory reporting to NPD) according to the petroleum legislation. This is where Diskos gets access to relevant data, and can make it available for public use as soon as the confidentiality period has expired (Diskos, 2017). Data accessible from Diskos include:

- Production data
- Well data
- Seismic data

Well data is the main focus area when working with RTDD. This includes mud logs, drilling reports and completion reports, which have been regularly used in this master thesis.

In order to download the desired data from Diskos, one needs to sign in as a member to the data base. At NTNU there are a limited number of people with access to Diskos because of copyright reasons. Only one master student was granted access to Diskos. Therefore, he was the main responsible for downloading the raw RTDD files to the drilldb\$ database during the cleaning project. Because the Diskos database is highly confidential, no pictures or screenshots of the data acquisition process can be published, together with no detailed information about the wells and data available.

6.3 Cleaning of data and categorization

Since different companies use different set-ups in their mud logging data, the preparation and cleaning process of the raw RTDD files was challenging. For the files to be compatible with the log viewer, they need to be of a certain format; Figure 6.2 shows the correct format, while Figure 6.3 shows an incompatible one:

	A	B	C	D	E	F	G	H
1	DATE,"TIME","LOGTIME","ACTC","BDIA","DBTM","DBTV","DMEA","DVER","RSU","RSD","ROP","BPOS","HKL							
2	dd-mmm-yy, hh:mm:ss, s, , IN, M, M, M, M, M/S, M/S, M/HR, M, TON, TON, KNM, RPM, RPM, HR, HR, REV, I							
3	03-Mar-05," 11:30:01 "	,794316601,-9999,-9999,2515.3759765625,-9999,2529.525146484375,2033.77471						
4	03-Mar-05," 11:30:06 "	,794316606,-9999,-9999,2515.658447265625,-9999,2529.525146484375,2033.774						
5	03-Mar-05," 11:30:11 "	,794316611,-9999,-9999,2515.92529296875,-9999,2529.525146484375,2033.7747						
6	03-Mar-05," 11:30:16 "	,794316616,-9999,-9999,2516.071533203125,-9999,2529.525146484375,2033.774						
7	03-Mar-05," 11:30:21 "	,794316621,-9999,-9999,2516.205078125,-9999,2529.525146484375,2033.774710						
8	03-Mar-05," 11:30:26 "	,794316626,-9999,-9999,2516.4541015625,-9999,2529.525146484375,2033.774710						
9	03-Mar-05," 11:30:31 "	,794316631,-9999,-9999,2516.649169921875,-9999,2529.525146484375,2033.774						
10	03-Mar-05," 11:30:36 "	,794316636,-9999,-9999,2516.8056640625,-9999,2529.525146484375,2033.774710						
11	03-Mar-05," 11:30:41 "	,794316641,-9999,-9999,2516.890380859375,-9999,2529.525146484375,2033.774						
12	03-Mar-05," 11:30:46 "	,794316646,-9999,-9999,2516.9931640625,-9999,2529.525146484375,2033.774710						
13	03-Mar-05," 11:30:51 "	,794316651,-9999,-9999,2517.149658203125,-9999,2529.525146484375,2033.774						

Figure 6.2: RTDD from well 33/12 B-40 DT2 with a format compatible with the log viewer.

For the raw RTDD file to be compatible, the date format needs to be dd-mmm-yy and time format in hh:mm:ss. In addition, these columns must be separated by -,"-. This is also valid for the caption row. The rest of the parameters is separated by -,-. When opened in Excel, all parameters, units and numbers need to be arranged in the first column. Consequently, the data has to be rearranged and divided into cells before Excel can be applied for further calculation purposes.

	A	B	C	D	E	F	G	H
1	TIME,"ACTC","BDIA","DBTM","DBTV","DMEA","DVER","RSU","RSD","ROP","BPOS","HKL","WOB","TRQ","RF							
2	S, , IN, M, M, M, M, M/S, M/S, M/HR, M, TON, TON, KNM, RPM, RPM, HR, HR, REV, BAR, BAR, BAR, BAR, BAF							
3	722260800,-9999,-9999,3629.7664550781251,-9999,3629.775634765625,2637.4170362,-9999,-0.50239396:							
4	722260805,-9999,-9999,3629.8064941406251,-9999,3629.814208984375,2637.4589982000002,-9999,-0.584							
5	722260810,-9999,-9999,3629.8448730468749,-9999,3629.8525390625,2637.4977327999995,-9999,-0.6786							
6	722260815,-9999,-9999,3629.8892578125001,-9999,3629.8984375,2637.5350848000003,-9999,-0.4875908!							
7	722260820,-9999,-9999,3629.9292968750001,-9999,3629.93701171875,2637.5761255999996,-9999,-0.157!							
8	722260825,-9999,-9999,3629.9659179687501,-9999,3629.97314453125,2637.5867320000002,-9999,0,29.17							
9	722260830,-9999,-9999,3629.97314453125,-9999,3629.97314453125,2637.5867320000002,-9999,0.250522							
10	722260835,-9999,-9999,3629.97314453125,-9999,3629.97314453125,2637.5867320000002,-9999,7.789663							
11	722260840,-9999,-9999,3629.5510742187498,-9999,3629.97314453125,2637.5867320000002,-9999,6.8756							
12	722260845,-9999,-9999,3628.9234863281249,-9999,3629.97314453125,2637.5867320000002,-9999,2.3626							
13	722260850,-9999,-9999,3628.7294921875,-9999,3629.97314453125,2637.5867320000002,-9999,0,23.2016							

Figure 6.3: RTDD from well 33/12 B-37 AT2 with an incompatible format for the log viewer.

The raw RTDD files that are incompatible with the log viewer can, for instance, follow the layout seen in Figure 6.3. Not only are incorrect separation characters used to distinguish each number, but the time format is either not adequate. Instead of the hh:mm:ss/dd-mmm-yy format, time is defined by the UNIX system, which is equivalent to the number of seconds that have elapsed since 00:00:00, Thursday, 1st of January 1970. Therefore, this file needs to undergo a cleaning process where the format is changed to the one above, before it can be opened in the log viewer.

In total, there exist six different formats of the raw RTDD files, each with different, defect set-ups. For the cleaning process to be more efficient and transparent, all formats were distinguished and categorized as described in Table 6.1:

Table 6.1: List of raw RTDD formats, and what makes them incompatible with the log viewer.

File Type	Format Properties
0	Correct format
1	No header, missing "-" and space as separation, format date and time missing
2	No header, First column of information, missing "-", No units ahead of data, UNIX-time
3	Similar to file type 2, only that mnemonics are hidden
4	Similar to file type 1, only that the headers are placed wrong and the date format is wrong
5	UNIX-time

Files of incorrect format (File type 1-5) therefore had to be cleaned and the properties that are unreadable by the log viewer had to be reformatted. This was done with the MATLAB software by another master student at NTNU, Clement Pierre Jean Donne. My task in this cleaning process, was to go through all Type 0 files, open them in the log viewer, and check that everything was compatible and that the RTDD was sufficient. Most of the RTDD files from the cleaning project are now stored in the updated drilldb\$-database, applicable with the log viewer. A full overview can be found in the wells_database folder in drilldb\$.

6.4 Selection of RTDD-files

When selecting wells that were to be investigated and tested against the model, the end-of-well reports were used as a starting point. Most of them contained detailed information about the drilling process and which problems and failures were encountered during the operations. It was therefore possible to search for drilling failures related to lost circulation and influxes, and wells of interest could be found more easily. Out of the ~160 RTDD-files that were cleaned, and with EoW-reports, about 26 wells experienced lost circulation, influxes or both to some extent. However, none of the RTDD-files from the time slots with these failures were possible to procure. Either, the EoW-reports contained information on the wrong wellbores, or the RTDD-files and the reports did not conform. Also, some RTDD-files were in a TIF-format, not yet compatible with the log viewer. It was therefore clear that most of the wells from the 90-ies had belonging EoW-reports, and no RTDD-files, while newer drilled wells only existed with RTDD-files and no EoW-reports. The wells with relevant failures found in the database were therefore useless, as no RTDD existed at the time those failures occurred.

However, there was one exception; well 1A was the only newer drilled well that had both RTDD and a belonging final well report. In addition, it was of great luck that lost circulation was one of the failures encountered in the actual well. This made it a good test well for the model, although no kick incidents occurred.

The final well report of well 1A contained information on BHA-setup, tools, well schematics and daily descriptions of operations performed on the rig. Together with RTDD and necessary parameters such as hole depth, bit depth, mud pump flow rates, ROP and active tank volumes, the model was provided with the required data for testing purposes.

7. Model evaluation

Even though the model has been made upon several assumptions, the final, modelled TVA-values correlate well with the true TVA measurements. This is seen from several intervals where the model was tested. A good example is an incident that occurred at $\sim 7:00$ on the 8th of February 2006, in well 1A. In the beginning, the model correlates well with the true TVA measurements, until the real TVA graph suddenly decreases (see Figure 7.1) compared to the model, indicating that more mud is lost than what is theoretically estimated. When looking into the final well report, it is stated that lost circulation occurred during drilling of this interval. The model therefore successfully detected lost circulation, as it revealed deviations between the theoretical and actual mud tank level.

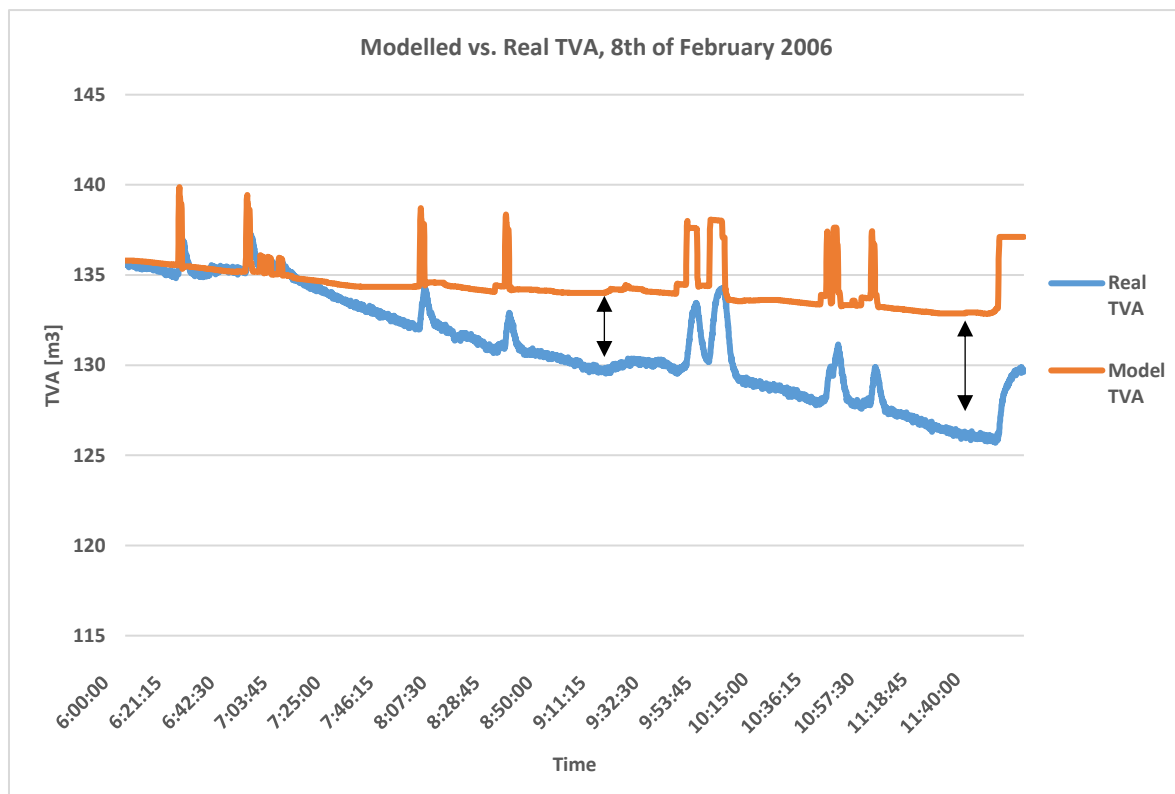


Figure 7.1: The model tested over an interval on the 8th of February 2006, from 6:00 to 12:00 in well 1A, reveals lost circulation (see black arrows that shows where mud is lost). The model is represented with an orange graph, and the real TVA measurements in blue.

In the final well report, it is stated that the losses were caused because of excessive torque and ECD.

Another interesting example is taken from an earlier interval: from 5th of February 2006 at 22:20 to 6th of February 2006 at 04:00 (see Figure 7.2). This interval also experiences a steeper decrease in the real mud tank volume.

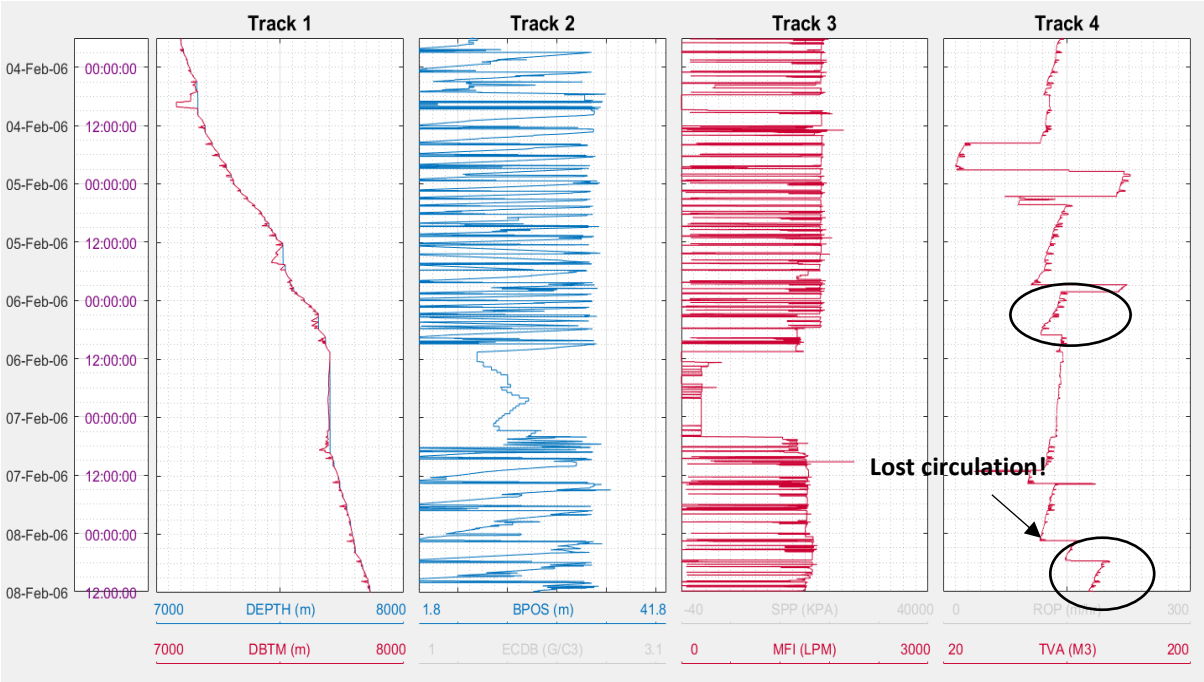


Figure 7.2: In track 4 the TVA-levels indicate two areas where the mud level is decreasing more drastically (black circles).

In Figure 7.3, the model was applied on the first interval.

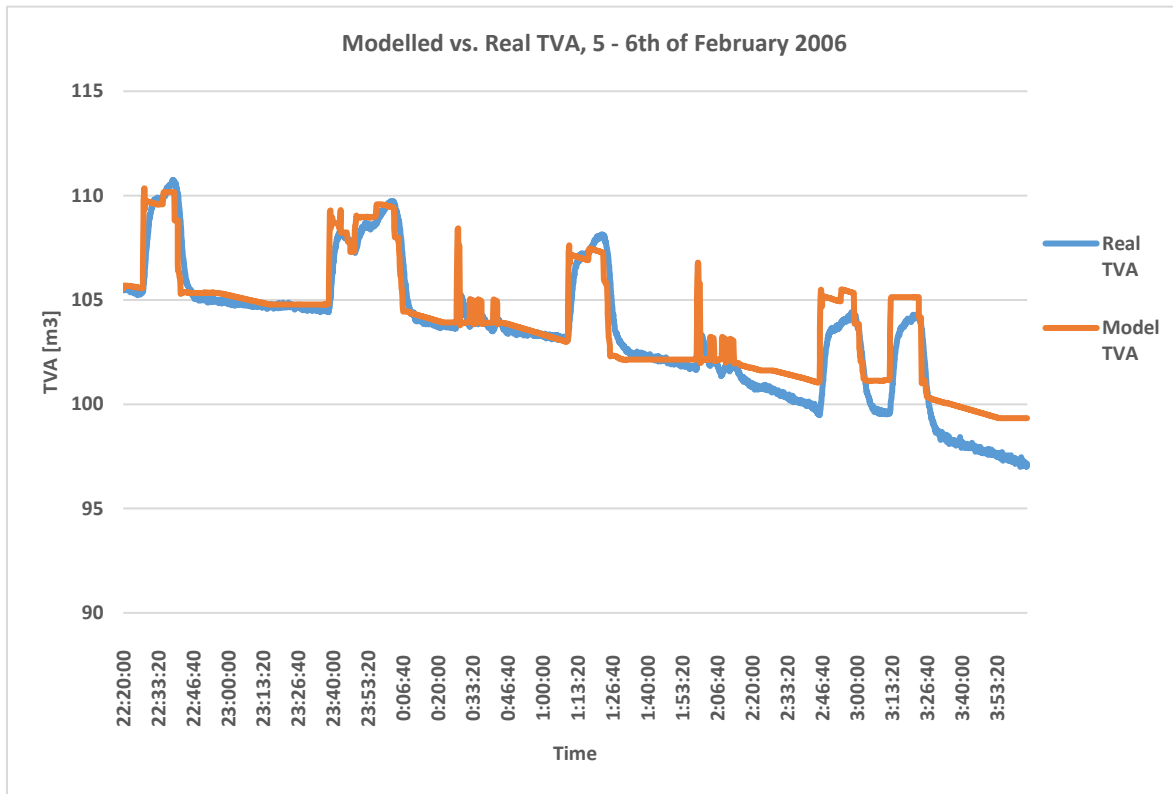


Figure 7.3: Observed TVA compared with modelled TVA. At 2:15, lost circulation is detected.

The model follows the observed TVA-graph closely until approximately 2:15, where the observed mud volume level starts to decrease more rapidly. Because no information could be found in the final well report whether lost circulation was occurring in this interval, other explanations were investigated.

One possible reason for the observed mud tank level to suddenly decrease with a steeper slope, could be that the drill string rotation (RPM) was high in the time-interval corresponding to rapid mud tank decrease. This would cause more cuttings settled on the low-side of the horizontal hole section to be suspended in the mud and transported out of the well (causing more mud loss). By applying RPM in the log viewer of the RTDD over the actual time span, the following can be observed:

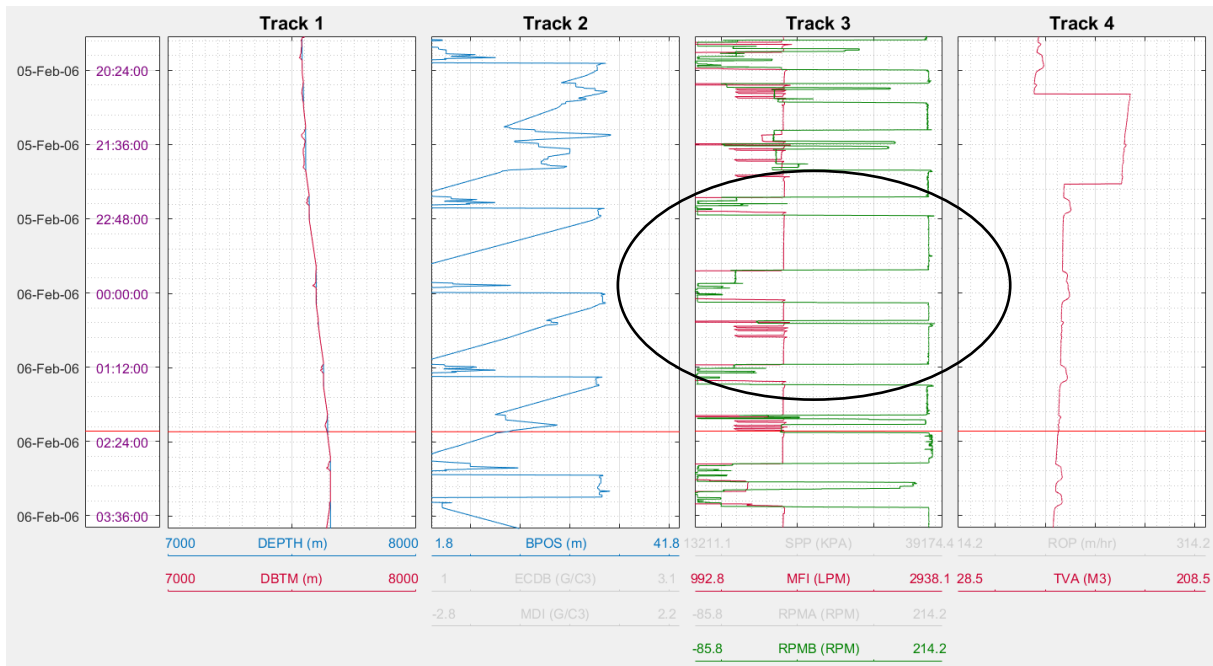


Figure 7.4: RTDD with TVA in track 4, and RPM in track 3 (green). The red, horizontal line is indicating hour 2.15.

Since lag-time has to be included (117 minutes in model, slightly more in a realistic situation), one can observe in Figure 7.4 that the RPM is kept high for two longer intervals before the decrease in mud tank level can be seen (approximately around 00:00, see black circle in Figure 7.4). However, the RPM was stable on a high speed before this as well, so it is difficult to say whether longer intervals with high RPM is of importance.

On the other hand, the detailed reporting from this section in the final well report was not of very good quality, and it could be a possibility that lost circulation occurred, but was not reported. This section was later plugged and side tracked because of problems, and lost circulation was one of them, as the ECD was three points higher than expected throughout the whole section. The risk of lost circulation was therefore high.

Last, one can discuss the adjustments that are being done. Especially towards the end of the section, right before the lost circulation situation arises (see Figure 7.5) - whether these are made to account for ongoing losses, and that lost circulation occurs other places than stated in the final well report, as the model could indicate.

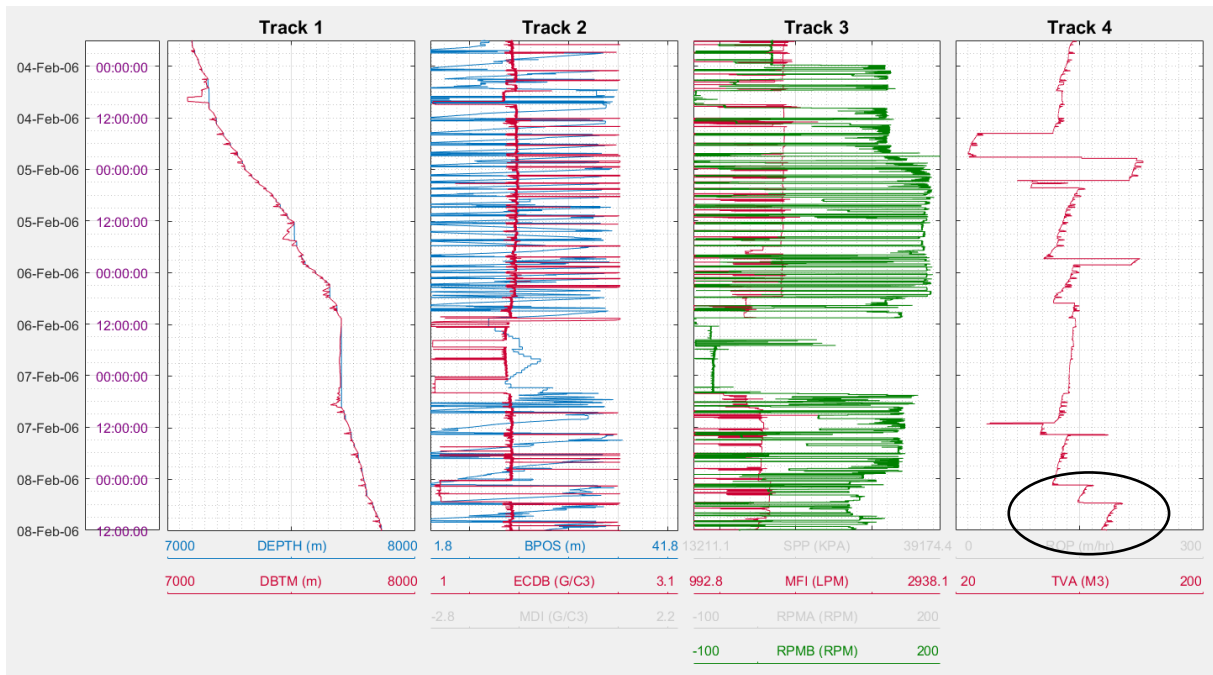


Figure 7.5: Several adjustments of the TVA are made in the last part of the section, near the lost circulation area (see black circle).

8. Self-assessment

The evaluation of the model confirmed that it was successful in detecting instabilities in the surface volume. It also revealed several uncertainties and aspects that could be improved for a future model. This chapter is divided into three subchapters:

- Model performance
- Data quality and uncertainty
- Future work → Improvements of thesis work on basis of self-assessment

8.1 Model performance

The model managed to detect lost circulation and the indications were clear and significant. However, the difference between modelled values and observed TVA measurements were sometimes increasing, also without reliable information about an ongoing lost circulation situation. Since the final well report stated that high ECD was an ongoing problem throughout the section, there could be reasons to believe the model was right over other intervals as well. Some of the sharp mud losses were difficult to explain from other available parameters, like high RPM, which could be another reasonable assumption.

When it comes to the accuracy of the model, several simplifying assumptions were made. The assumption that the cuttings travel with the same velocity as the drilling fluid was not realistic, and gave a shorter lag-time than expected. During each connection, the pumps are turned off, and cuttings start slipping down until the pumps are turned on again, in addition to general gravity forces. However, information about the sizes and shapes of the cuttings were not available, and a correct slip velocity would have been difficult to find. Still, one should be aware of it, especially in the lag-time calculations.

Furthermore, the accuracy of how much mud was lost as a “film” surrounding the cuttings over the shale shaker, is uncertain. This depends on the surface area of the cuttings. In other words, one large cutting would have a different mud film than if the same cutting was

divided into several, smaller cuttings. Moreover, the volume of formation that is drilled will be larger when taken to surface since the effective porosity is made larger when dug out.

When it comes to the sudden increases of TVA-level, as the mud pumps are shut down, on the modelled values, some of them are a bit high (see Figure 7.1 and Figure 7.3). This can be explained by the fact that it is a simplified model. As soon as the flow rate is zero, the volume increase in the model is set to V_{max} . However, in a realistic situation, it is not certain that all of the fluid will manage to flow back -this is dependent on for how long the pumps are turned off. In addition, the viscosity might vary in a realistic model, which affects flowback from the mud pumps through surface lines greatly, as more viscous fluid takes longer flowing through pipelines and tanks. Lastly, one can question the accuracy of the trendline from the ΔTVA and V_{max} calculations (see Figure 5.19).

In the end, the overall performance of the model was good, and if used during drilling of well 1A, it would have managed to detect the lost circulation incident.

8.2 Data quality and uncertainty

Because RTDD is sampled from a drilling rig, and relies on sensors and other machinery and technical solutions, there is always a chance of poor data quality, uncertainties and wrong measurements. However, in the present thesis, it is assumed that the calibration-process is executed, leading to acceptable quality. Among large data amounts, only those of great importance are included. Many parameters would not affect the results to any great extent either. Still, poor data quality occurs occasionally. For instance, the ECD measurements from well 1A seemed to be a bit off. Each time the pumps were turned on, the ECD increased from 1,69 g/cm³ to 2,5 g/cm³. This does not sound logical, so the chance of poor data quality is large. Luckily, this did not affect any results.

Moreover, as the measurements were taken every fifth second, there is always a chance of missing specific measurements and influence on the accuracy. For instance, if bit depths are not close to 100% accuracy, this could impact steel displacement calculations. However, this did probably not affect the model particularly much.

The quality of the final well report used in this master thesis was fairly good. A good selection of necessary drilling parameters was given, however some detailed values had to be estimated, as they were missing. In addition, some of the information given was inaccurate and even wrong (when compared to the belonging RTDD). Again, it is important to be critical to all information given, and double check dates, depths, parameters and other data. Perhaps one could also ask the relevant oil company if any supporting documents are available.

Lastly, the RTDD collected from Diskos and the EoW-reports downloaded from the associated wells during the data acquisition process, proved to mismatch. Typically, the RTDD were relatively recent, with data from wells drilled after year 2000, while the EoW-reports were reporting from mother wells drilled during the 1980-ies and 1990-ies (same geological area, but different wells). This made the process of finding good wells, with relevant failures and high-quality information, difficult.

8.3 Future work → Improvements of thesis work on basis of self-assessment

Future work will be related to improving the model and later test it on more wells to better check its performance. For improvement, the model should take in more parameters, so that several properties can be included and accuracy increased. Some of these include:

1. Filter cake.
2. Gas content in mud.
3. Fluid expansion due to temperature differences.
4. Heave motions.
5. A cuttings transport model involving the effect of RPM.
6. Improved lag-time model which includes slip velocity.

The accuracy of the RTDD is good, and not necessary to improve. It is therefore important to continue being critical about the results, and try to investigate whether they are useable or not. Whenever the data quality is questionable, one can insert logical checks to reveal possible bad data. Because there is a mismatch between RTDD and EoW-reports, one could contact the relevant oil companies to obtain more data, like reports and special investigations, to support the EoW-reports.

Additionally, it will be easy to include trip tank measurements in the model. By differentiating between drilling and tripping operations, it is possible to calculate expected trip tank and mud tank values accordingly. Especially during tripping, this is beneficial, as the trip tank is smaller, and can easier detect volume changes.

Lastly, the model should be upgraded and made more user-friendly by selecting the programming language MATLAB. In present work, RTDD had to be copied manually from the original well data-file, and parameters related to lag-time had to be implemented partly manually. Making the whole model automatic would be a great improvement.

9. Conclusion

The model proved to be successful in detecting lost circulation, which means it would detect pit gain as well. However, kicks were not seen in the data.

The conclusions of the project are as follows:

- The model indicated several intervals where more mud was lost than theoretically calculated. With available data and information for the project, the losses were interpreted as lost circulation.
- Several constants representing process parameters were found from observed trend lines. These constants made the model less uncertain.
- The model is simplified, and several assumptions were made. However, it excluded indirect physical parameters like heave, RPM, fluid expansion due to temperature differences, volume increase because of gas trapped in drilling fluid and mud lost to “filter cake”.
- Of the wells downloaded and investigated from Diskos, well 1A was the only well containing RTDD, combined with a final well report, that encountered volume control problems.
- The quality of the RTDD was mostly good, and the quality of the final well report was fairly good.
- For future improvements, the model must be made more advanced and should be tested on more wells, preferably with failure incidents. In addition, it could be made more user-friendly and automatic.

The improvements may be achieved through:

- Consider more parameters and properties.
- Improve lag-time model.
- Improve cuttings generation model.
- Implement the model in MATLAB.

10. Nomenclature

$P_{\text{hydrostatic}}$	Pressure exerted by hydrostatic column [bar]
ρ_{mud}	Density of mud/drilling fluid [kg/m^3]
g	Acceleration of gravity [m/s^2]
h	Height [m]
$P_{\text{formation}}$	Pressure exerted by formation [bar]
$V_{\text{steel in}}$	Volume increase caused by steel inserted in the well [m^3]
$V_{\text{steel out}}$	Volume decrease caused by steel removed from the well [m^3]
$V_{\text{cuttings+film}}$	Volume of cuttings removed from the well together with volume of mud sticking onto the cuttings [m^3]
$V_{\text{pump on}}$	Volume decrease caused by mud flow in surface lines when pumps are started [m^3]
$V_{\text{pump off}}$	Volume increase caused by mud flow in surface lines when pumps are shut down [m^3]
$V_{\text{adj_up}}$	Increasing volume changes caused by mud level adjustments [m^3]
$V_{\text{adj_down}}$	Decreasing volume changes caused by mud level adjustments [m^3]
ΔV_{pit}	Total volume change in mud pit [m^3]
Cap_{dp}	Steel capacity of drill pipe [m^2]
DBTM	Bit depth [mMD]
DMEA	Hole depth [mMD]
t	Time step counter [s]
t_{lag}	The delay of volume changes in mud tank caused by cuttings velocity up through wellbore [min]
K_{film}	A constant indicating how much mud is sticking to the cuttings surface in the cleaning system
M_{pit}	Mass in mud pit
V_{max}	The maximum volume increase/decrease in the pit caused by turning off/on the mud pumps [m^3]
q_p or q_{pump}	Mud-flow in (MFI) [l/min & m^3/min]
A_{bit}	Cross-sectional area of the hole/bit [m^2]
V_{ann}	Annular volume [m^3]
q_{hole}	Rate in which hole is drilled [m^3/min & $\text{m}^3/5\text{s}$]

11. Abbreviations

Bottom Hole Assembly	BHA
Block Position	BPOS
Bit Depth (Measured Depth)	DBTM
Hole depth (Measured Depth)	DMEA
Drill Pipe	DP
Effective Circulation Density at Bit	ECDB
Equivalent Circulating Density	ECD
End of Well	EoW
Inner Diameter	ID
Lost Circulation Material	LCM
Litre Per Minute	LPM
Measured Depth	MD
Mud density in	MDI
Mud Flow In	MFI
Non Productive Time	NPT
Outer Diameter	OD
Open Ended	OE
Open hole	OH
Pull Out Of Hole	POOH
Run In Hole	RIH
Rotary Kelly Bushing	RKB
Rate Of Penetration	ROP
Rotations Per Minute (Average rotary speed)	RPM
Real Time Drilling Data	RTDD
Strokes Per Minute	SPM
Stand Pipe Pressure	SPP
Tagged Image File Format	TIF
Active Tank Volume	TVA
Well head	WH

12. References

- BRECHAN, B. A. 2015. TPG4210 Drilling Engineering - Compendium. NTNU, Department of Geoscience and Petroleum
- CAYEUX, E., DAIREAUX, B., DVERGSNES, E. & SAELEVIK, G. 2012. Early Symptom Detection Based on Real-Time Evaluation of Downhole Conditions: Principles and Results from several North Sea Drilling Operations. *SPE Intelligent Energy International*. Utrecht, The Netherlands: Society of Petroleum Engineers.
- CHMELA, B., ABRAHIMSEN, E. & HAUGEN, J. Prevention of Drilling Problems Using Real-Time Symptom Detection and Physical Models. *Offshore Technology Conference Asia*. Kuala Lumpur, Malaysia: Offshore Technology Conference.
- CORINA, A. N. 2017. User Guide: Real-Time Drilling Data (RTDD) Log Viewer. Trondheim, Norway: Norwegian University of Science and Technology.
- DISKOS, N. P. D. 2017. *About Diskos* [Online]. Available: www.diskos.no [Accessed 5th May 2017].
- GAURINA-MEDJIMUREC, N. & PASIC, B. 2014. *Risk Analysis for Prevention of Hazardous Situations in Petroleum and Natural Gas Engineering*, USA, Engineering Science Reference.
- HALLIBURTON 2013. The Halliburton Baroid Ecosystem - Lost Circulation. *In*: HALLIBURTON, L. C. (ed.) *YouTube*. YouTube.com: YouTube.
- LAKE, L. W. & MITCHELL, R. F. 2006. *Petroleum Engineering Handbook*, Society of Petroleum Engineers.
- LAVROV, A. 2016a. Chapter 5 - Mechanisms and Diagnostics of Lost Circulation. *Lost Circulation*. Boston: Gulf Professional Publishing.
- LAVROV, A. 2016b. Chapter 6 - Preventing Lost Circulation. *Lost Circulation*. Boston: Gulf Professional Publishing.
- MITCHELL, R. F. & MISKA, S. Z. 2010. *Fundamentals of Drilling Engineering*, Society of Petroleum Engineers.

NAYEEM, A. A., VENKATESAN, R. & KHAN, F. 2016. Monitoring of down-hole parameters for early kick detection. *Journal of Loss Prevention in the Process Industries*, 40, 43-54.

SCHOOL OF PETROLEUM ENGINEERING, U. O. N. S. W. 2014. Kick detection. *Well Control and Blowout Prevention PTRL 6025*.

13. Figures

Figure 2.1: The principle behind IRIS' model, which compares real-time sensor data with calculated model data (Chmela et al.).....	3
Figure 2.2: It can take several minutes from the pumps are shut down until all of the fluid stored in the surface lines flows back to the active tank, which causes an apparent gain (Cayeux et al., 2012).....	5
Figure 2.3: The red circle indicates where the models (green graph) discover an abnormal mud level increase when compared to the measured tank volume (blue graph) (Cayeux et al., 2012).....	6
Figure 3.1: Kicking well: Left: a balanced situation where the hydrostatic pressure is higher or equal to the formation pressure; no influx. Middle: kick situation, where the hydrostatic pressure is too low to withstand the formation pressure. Right: lost circulation.....	9
Figure 3.2: Example showing how a drill break looks on the Drilling rate vs. Well depth plot.....	10
Figure 3.3: An overview of the circulation system showing how the mud pits are connected to the well. The fluid level in the mud pits is monitored to check for volume increases by the level indicators (Brechan, 2015).....	12
Figure 3.4: An example of a hook load plot. In the event of an influx, the hook load will increase as a reaction to smaller buoyancy force provided by the lighter mud in the wellbore. (WellPlan™ software).....	13
Figure 3.5: A single drill pipe. Each end consists of a tool joint; one pin end and one box end, which will affect the volume displacement in mud (Brechan, 2015).....	14
Figure 3.6: Trip tank arrangement on a drilling rig (Brechan, 2015).....	15
Figure 3.7: Overview of the three trip tank arrangements; 1. Passive type (based on the u-tube principle), 2. Semi-passive type (based on gravity forces) and 3. Active type (based on a centrifugal pump (School of Petroleum Engineering, 2014).....	16
Figure 4.1: Lost circulation zone being drilled (Halliburton, 2013).....	17
Figure 4.2: Overview of lost circulation zones (Gaurina-Medjimurec and Pasic, 2014).....	20
Figure 4.3: How lost circulation zones can be detected through temperature surveys; first, mud temperature is measured downhole after equilibrium with the formation is established. Then, fresh mud is circulated, and a new temperature measurement is done. From the black dotted graph (temperature of fresh mud), it is possible to see a sharp jump in temperature at the zone of loss (Gaurina-Medjimurec and Pasic, 2014).....	22
Figure 4.4: Improper fracture bridging can be seen on the left side of the hole, and proper fracture bridging to the right. This illustrates the importance of choosing the correct granular/fibrous/flaked sizes of LCM (Gaurina-Medjimurec and Pasic, 2014).....	24

Figure 4.5: Operational procedure of chemical sealant placement. The mechanism is similar for setting plugs/pills. The drillstring is lowered to the loss area, where the pill is pumped into the formation or the chemical sealant is activated (Gaurina-Medjimurec and Pasic, 2014).....	24
Figure 5.1: Overview of the mud circulation system, and the parameters that affect the mud pit level.....	26
Figure 5.2: Control volume of the mud pit showing mass flow in and mass flow out.....	28
Figure 5.3: Real TVA measurements versus modelled values. From well 1A on the 5 th of February 2006 from 21:00 to 0:00.....	30
Figure 5.4: The volume change caused by drilled cuttings will be felt at surface after a given “lag-time”	34
Figure 5.5: Track 3 shows the flow rates from the mud pumps. As can be observed, it varies between three values during the drilling operations (indicated by the black arrows).....	34
Figure 5.6: Five intervals were found out from the TVA measurements in track 4 (black circles).....	36
Figure 5.7: The real TVA measurements vs. the modelled one for a 9” hole. From 3 rd - 4 th of February 2006, 20:00 to 05:10. Two different K_{film} -values were found for making results more accurate.....	38
Figure 5.8: The real TVA measurements vs. the modelled one for a 9” hole. From the 5 th of February 2006, 04:20 to 14:05.....	39
Figure 5.9: The real TVA measurements vs. the modelled one for a 9” hole. From the 5 th – 6 th of February 2006, 22:20 to 04:05.....	39
Figure 5.10: The real TVA measurements vs. the modelled one for a 9” hole. From the 7 th – 8 th of February 2006, 13:55 to 01:00.....	40
Figure 5.11: The real TVA measurements vs. the modelled one for a 9” hole. From the 8 th of February 2006, 06:00 to 11:45.....	41
Figure 5.12: The real TVA measurements vs. the modelled one for a 9” hole. From the 4 th of February 2006, 13:30 to 13:52.....	41
Figure 5.13: Overview of the condeep platform’s well configuration.....	43
Figure 5.14: The pump flow rate is found in track 3. Observe that the pumps are shut down between 05:40 and 8:45 on the 4 th of February 2006 (black box).....	44
Figure 5.15: Time vs. TVA and MFI (q_{pump}) on the 4 th of February from 05:00 to 07:00.....	45
Figure 5.16: Time vs. TVA and MFI (q_{pump}) on the 4 th of February from 21:00 to 23:00.....	46
Figure 5.17: Time vs. TVA and MFI (q_{pump}) on the 6 th of February from 10:00 to 12:00.....	46
Figure 5.18: Time vs. TVA and MFI (q_{pump}) on the 8 th of February from 10:00 to 12:00.....	47

Figure 5.19: Trendline describing the relationship between volume stored in surface lines, Δ TVA, and pump flow rate, q.....48

Figure 5.20: Track 4 shows the active tank volume (TVA), where several adjustments can be observed inside the black circles.....50

Figure 6.1: An outcrop of the template script.....53

Figure 6.2: RTDD from well 33/12 B-40 DT2 with a format compatible with the log viewer.....56

Figure 6.3: RTDD from well 33/12 B-37 AT2 with an incompatible format for the log viewer.....57

Figure 7.1: The model tested over an interval on the 8th of February 2006, from 6:00 to 12:00 in well 1A, reveals lost circulation (see black arrows that shows where mud is lost). The model is represented with an orange graph, and the real TVA measurements in blue.....61

Figure 7.2: In track 4 the TVA-levels indicate two areas where the mud level is decreasing more drastically (black circles).....62

Figure 7.3: Observed TVA compared with modelled TVA. At 2:15, lost circulation is detected.....63

Figure 7.4: RTDD with TVA in track 4, and RPM in track 3 (green). The red, horizontal line is indicating hour 2.15.....64

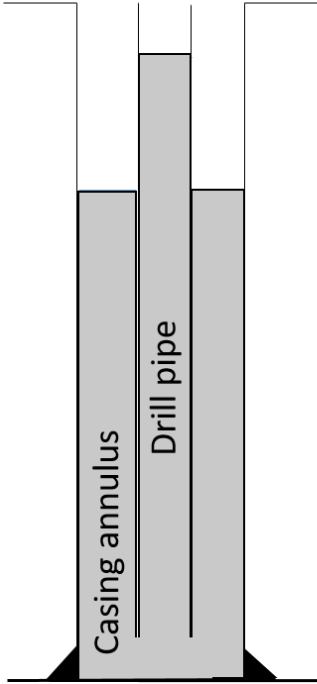
Figure 7.5: Several adjustments of the TVA are made in the last part of the section, near the lost circulation area (see black circle).....65

14. Tables

Table 5.1: Some of the most important parameters and calculations of the theoretical model.....	29
Table 5.2: Steel displacement calculations for moving drill pipe.....	31
Table 5.3: Calculations of average pump flow rate in each section given in litres per minute.....	35
Table 5.4: Annular volume and lag-time calculations for period 1 with $q_{\text{pump}} = 1,53 \text{ m}^3/\text{min}$. Average lag-time for period marked in red.....	35
Table 5.5: Lag-time for all three periods.....	36
Table 5.6: Calculations of theoretical mud volume needed to fill drilled volume.....	37
Table 5.7: Based on ROP, the hole volume drilled was calculated together with cuttings concentration at the bottom of the well.....	38
Table 5.8: Overview of K_{film} -values from the intervals investigated.....	42
Table 5.9: Results of TVA level increase after pump shut-off.....	47
Table 6.1: List of raw RTDD formats, and what makes them incompatible with the log viewer.....	58

Appendix A: U-tube effect

1. Realistic model



2. U-tube model

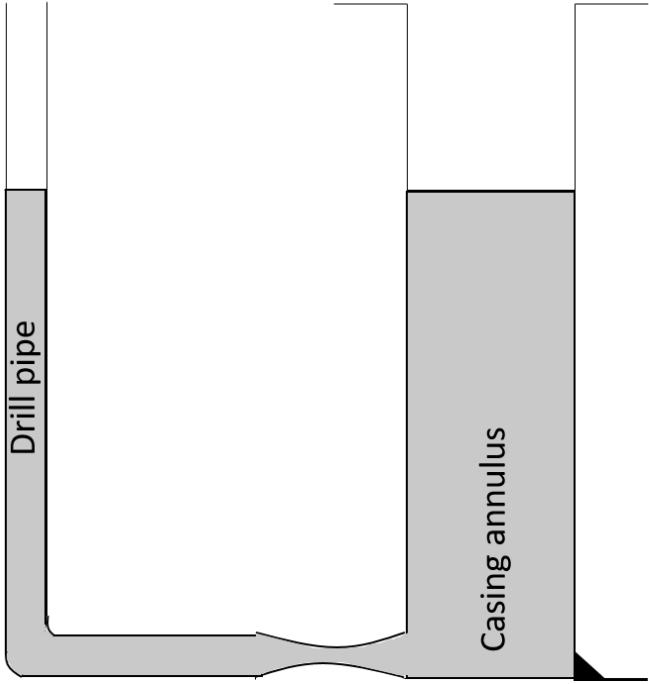


Figure A1: Model 1 shows a normal well schematic, while model 2 shows the U-tube effect.

The U-tube effect is a model used for understanding constant bottom hole pressure, and pressure communications between the drill pipe and the annulus. As long as the flap valve inside the drill string is open, there will be pressure interactions between the two channels, and an equilibrium will be established. Based on the densities of the fluids present, the heights of each fluid column will change accordingly, in order to keep the bottom hole pressure constant. For example, if the drill pipe contains a heavy slug pill, this will affect the fluid column in the annulus. However, if the densities are the same, there will be no difference in column height. To the right in Figure A1 it is possible to see how the two channels forms a “U”-shape, which explains the name “U-tube effect”.

Appendix B: Log viewer template

```
% TRACKS TEMPLATE -- DO NOT CHANGE THE VARIABLE NAME

% For each curve track, it contains field:

% 1. Name = the name of the track preferred by the users

% 2. Curves = the curves assigned in each track

% 3. XScale = linear or logarithmic axes for the track

inputTrack = struct(...

    'Name', {'Track 1','Track 2','Track 3', 'Track 4'}

    },...

    'Curves', {{'DEPTH','DBTM'},...

                {'BPOS','ECD','MDI'},...

                {'WOB','TRQ'},...

                {'SPP','ROP','TVA'}}},...

    'XScale', {'linear','linear','linear','linear'});

% FOR CURVE PROPERTIES -- DO NOT CHANGE VARIABLE NAME

% These curve properties allow users to set preferred options for the

% curves. For default, type 'auto' in the input.

% If user wants to use all the defaulted properties, then set inputCurves

% as an empty matrix. inputCurves = [];

% 1. Name = the curves name. Note: the curves name must be the same

% with the curves name in inputTrack.

% 2. Unit = unit of the curves4

% Input : (unit string) | 'auto'
```



```

% 3. Min    = minimum value of the curves.

%          Input : (positive value) | 'auto'

% 4. Max    = maximum value of the curves.

%          Input : (positive value) | 'auto'

% 5. LineWidth = line width of the curves.

%          Input : (positive value) | 'auto'

% 6. LineColor = line color of the curves

%          Input : (RGB triplet) | 'auto'

%          RGB triplet is three-element row vector whose elements

%          specify the intensities of the red, green, and blue

%          components of the color. The intensities must be in the

%          range [0,1], for example, [0.4 0.6 0.7].

% An example to write inputCurve:

% inputCurves = struct('Name',{'HKLD','SPP'},...

%   'Unit',{'KGFm','bar'},...

%   'Min',{'auto',0},...

%   'Max',{200000,'auto'},...

%   'LineWidth',{'auto',0.8},...

%   'LineColor',{[0.000, 0.447, 0.741],[0.800, 0.000, 0.200]});

inputCurves = struct('Name',{'GR','BPOS','ROP'},...

    'Min',{0,0,0},...

    'Max',{200,'auto','auto'});

```

Published with MATLAB® R2016a

Appendix C: Capacities of drill pipes

CAPACITIES OF DRILL PIPES (continued)

Nominal size (in)	Nominal weight (lb/ft)	Upset	Grade	Thread	Tool joint		Volumes (1) (l/m)		
					OD (in)	ID (in)	Metal displacement	Capacity	Total displacement
4 1/2	20.00	IEU	E75	FH	6	3	4.11	6.60	10.71
4 1/2	20.00	IEU	X95	FH	6	2 1/2	4.24	6.52	10.76
4 1/2	20.00	IEU	G105	FH	6	2 1/2	4.24	6.52	10.76
4 1/2	20.00	EU	E75	NC50(IF)	6 3/8	3 5/8	4.10	6.71	10.81
4 1/2	20.00	EU	E75	NC50(IF)	6 5/8	3 5/8	4.19	6.71	10.90
4 1/2	20.00	EU	X95	NC50(IF)	6 3/8	3 1/2	4.19	6.69	10.88
4 1/2	20.00	EU	X95	NC50(IF)	6 5/8	3 1/2	4.28	6.69	10.97
4 1/2	20.00	EU	G105	NC50(IF)	6 3/8	3 1/2	4.19	6.69	10.88
4 1/2	20.00	EU	G105	NC50(IF)	6 5/8	3 1/2	4.28	6.69	10.97
4 1/2	20.00	EU	S135	NC50(IF)	6 5/8	3	4.37	6.59	10.97
5	19.50	IEU	E75	NC50(XH)	6 3/8	3 3/4	3.96	9.15	13.11
5	19.50	IEU	E75	NC50(XH)	6 5/8	3 3/4	4.05	9.15	13.19
5	19.50	IEU	X95	NC50(XH)	6 3/8	3 1/2	4.06	9.10	13.16
5	19.50	IEU	X95	NC50(XH)	6 5/8	3 1/2	4.15	9.10	13.24
5	19.50	IEU	G105	NC50(XH)	6 1/2	3 1/4	4.15	9.05	13.20
5	19.50	IEU	G105	NC50(XH)	6 5/8	3 1/4	4.19	9.05	13.24
5	19.50	IEU	S135	NC50(XH)	6 5/8	2 3/4	4.28	8.97	13.24
5	19.50	IEU	E75	5 1/2 FH	7	3 3/4	4.23	9.14	13.37
5	19.50	IEU	X95	5 1/2 FH	7	3 3/4	4.28	9.14	13.42
5	19.50	IEU	G105	5 1/2 FH	7	3 3/4	4.28	9.14	13.42
5	19.50	IEU	S135	5 1/2 FH	7 1/4	3 1/2	4.44	9.08	13.52
5	25.60	IEU	E75	NC50(IF)	6 3/8	3 1/2	5.10	8.01	13.10
5	25.60	IEU	E75	NC50(IF)	6 5/8	3 1/2	5.19	8.00	13.18
5	25.60	IEU	X95	NC50(IF)	6 1/2	3	5.27	7.92	13.19
5	25.60	IEU	X95	NC50(IF)	6 5/8	3	5.32	7.91	13.23
5	25.60	IEU	G105	NC50(IF)	6 5/8	2 3/4	5.36	7.87	13.23
5	25.60	IEU	E75	5 1/2 FH	7	3 1/2	5.37	7.99	13.36
5	25.60	IEU	X95	5 1/2 FH	7	3 1/2	5.41	7.99	13.41
5	25.60	IEU	G105	5 1/2 FH	7 1/4	3 1/2	5.52	7.99	13.51
5	25.60	IEU	S135	5 1/2 FH	7 1/4	3 1/4	5.57	7.94	13.51
5 1/2	21.90	IEU	E75	5 1/2 FH	7	4	4.51	11.37	15.88
5 1/2	21.90	IEU	X95	5 1/2 FH	7	3 3/4	4.63	11.32	15.95
5 1/2	21.90	IEU	G105	5 1/2 FH	7 1/4	3 1/2	4.79	11.26	16.05
5 1/2	21.90	IEU	S135	5 1/2 FH	7 1/2	3	5.00	11.15	16.15
5 1/2	24.70	IEU	E75	5 1/2 FH	7	4	4.99	10.89	15.87
5 1/2	24.70	IEU	X95	5 1/2 FH	7 1/4	3 1/2	5.26	10.77	16.03
5 1/2	24.70	IEU	G105	5 1/2 FH	7 1/4	3 1/2	5.26	10.77	16.03
5 1/2	24.70	IEU	S135	5 1/2 FH	7 1/2	3	5.47	10.67	16.14
6 5/8	25.20	IEU	E75	6 5/8 FH	8	5	5.22	17.72	22.95
6 5/8	25.20	IEU	X95	6 5/8 FH	8	5	5.22	17.72	22.95
6 5/8	25.20	IEU	G105	6 5/8 FH	8 1/4	4 3/4	5.42	17.64	23.07
6 5/8	25.20	IEU	S135	6 5/8 FH	8 1/2	4 1/4	5.69	17.50	23.19
6 5/8	27.70	IEU	E75	6 5/8 FH	8	5	5.57	17.36	22.93
6 5/8	27.70	IEU	X95	6 5/8 FH	8 1/4	4 3/4	5.77	17.28	23.05
6 5/8	27.70	IEU	G105	6 5/8 FH	8 1/4	4 3/4	5.77	17.28	23.05
6 5/8	27.70	IEU	S135	6 5/8 FH	8 1/2	4 1/4	6.04	17.13	23.18

Appendix D: Casing sizes

Overview of the properties of the 9 5/8" casing.

Size – OD [in]	Weight [lbm/ft]	Grade	Wall Thickness [in]	ID [in]	Drift [in]	OD of Coupling [in]	OD special clearance coupl [in]	Collapse [psi]	Yield pipe body [1000 lbf]	Nom Weight Threads and Coupling [kg/m]	Capacity [l/m]	OE Displacement [l/m]	CE Displacement [l/m]
9,625	43,5	N-80	0,435	8,755	8,599	10,625	10,125	3810	1005	64,73	38,84	8,1	46,94
9,625	47	N-80	0,472	8,681	8,525	10,625	10,125	4760	1086	69,94	38,19	8,76	46,94
9,625	53,5	N-80	0,545	8,535	8,379	10,625	10,125	6620	1244	79,62	36,91	10,03	46,94
9,625	40	C-90	0,395	8,835	8,679	10,625	10,125	3250	1031	59,53	39,55	7,39	46,94
9,625	43,5	C-90	0,435	8,755	8,599	10,625	10,125	4010	1130	64,73	38,84	8,1	46,94
9,625	47	C-90	0,472	8,681	8,525	10,625	10,125	5000	1221	69,94	38,19	8,76	46,94
9,625	53,5	C-90	0,545	8,535	8,379	10,625	10,125	7120	1399	79,62	36,91	10,03	46,94
9,625	40	C-95	0,395	8,835	8,679	10,625	10,125	3320	1088	59,53	39,55	7,39	46,94
9,625	43,5	C-95	0,435	8,755	8,599	10,625	10,125	4120	1193	64,73	38,84	8,1	46,94
9,625	47	C-95	0,472	8,681	8,525	10,625	10,125	5090	1289	69,94	38,19	8,76	46,94
9,625	53,5	C-95	0,545	8,535	8,379	10,625	10,125	7340	1477	79,62	36,91	10,03	46,94
9,625	43,5	P-110	0,435	8,755	8,599	10,625	10,125	4420	1381	64,73	38,84	8,1	46,94
9,625	47	P-110	0,472	8,681	8,525	10,625	10,125	5300	1493	69,94	38,19	8,76	46,94
9,625	53,5	P-110	0,545	8,535	8,379	10,625	10,125	7950	171	79,62	36,91	10,03	46,94
10,75	32,75	H-40	0,279	10,192	10,036	11,75	-	8400	367	48,74	52,64	5,92	58,56
10,75	40,5	H-40	0,35	10,05	9,894	11,75	-	1390	457	60,27	51,18	7,38	58,56
10,75	40,5	J-55	0,35	10,05	9,894	11,75	11,25	1580	629	60,27	51,18	7,38	58,56
10,75	45,5	J-55	0,4	9,95	9,794	11,75	11,25	2090	715	67,71	50,17	8,39	58,56
10,75	51	J-55	0,45	9,85	9,694	11,75	11,25	2700	801	75,90	49,16	9,39	58,56
10,75	40,5	K-55	0,35	10,05	9,894	11,75	11,25	1580	629	60,27	51,18	7,38	58,56
10,75	45,5	K-55	0,4	9,95	9,794	11,75	11,25	2090	715	67,71	50,17	8,39	58,56
10,75	51	K-55	0,45	9,85	9,694	11,75	11,25	2700	801	75,90	49,16	9,39	58,56
10,75	51	C-75	0,45	9,85	9,694	11,75	11,25	3110	1092	75,90	49,16	9,39	58,56
10,75	55,5	C-75	0,495	9,76	9,604	11,75	11,25	3920	1196	82,59	48,27	10,29	58,56
10,75	51	L-80	0,45	9,85	9,694	11,75	11,25	3220	1165	75,90	49,16	9,39	58,56

(Brechan, 2015)